

ANTENNA ARRAYS AND CLASSICAL BEAMFORMING

4

The purpose of this chapter is to explain the basic concept of classical beamforming using an antenna array, where, like a flashlight beam, signal power can be directed in a desired direction. This is accomplished by a beamformer that adjusts the signals transmitted from the elements of an array so that they combine constructively at an intended receiver. The corresponding gain pattern, sometimes referred to as a beam or beam gain pattern, is derived and illustrated and some properties like maximum gain and width of the main lobe are described for commonly used configurations such as uniform linear and planar arrays.

The focus is on the free-space single-path propagation scenario introduced in Chapter 3. Results in this chapter will then serve as inputs to Chapter 5, where the setup will be extended by considering multipath propagation, multiple orthogonal frequency division multiplexing (OFDM) subcarriers, and multiple antennas at the receiver side as well. More specifically, Chapter 5 will formulate a multiple-input, multiple-output (MIMO) OFDM channel model based on the so-called array response vector introduced in the present chapter. This in turn will allow exploration of various multi-antenna techniques in Chapter 6.

Finally, a uniform planar array (UPA) of dual-polarized element pairs and the partitioning of such an array into an array of subarrays are introduced. The latter partitioning facilitates consideration of how to find a suitable number of radio chains as a function of the deployment, as described in Chapters 13 and 14.

4.1 INTRODUCTION

An antenna array is set of antennas commonly organized in a structure such as an array of rows and columns. An antenna array can be used for both transmission and reception. By transmitting different versions of the same signal from all the antennas, the signal's amplification, referred to as gain, can be controlled so that the gain is different in different directions. Rather than spreading the signal power over an entire cell, the signal power can be directed to where the intended user is located and even be reduced in other directions to avoid interfering other users. Similarly, when the antenna array is used for reception, the gain in the direction of where the user is located can be increased so that the received signal power is increased.

The signals transmitted from different antennas are converted into electromagnetic waves that combine in the air. Considering a receiver located at some distance right in front of the transmitting antenna array, the propagation path lengths from the different antennas to the receiver are essentially the same and if the same signal is transmitted from all the antennas, the waves will add constructively at the receiver. With N antennas, the amplitude of the resulting wave is N times higher

than the amplitude for a single antenna. For the same total transmission power, the amplitude per antenna is however downscaled with a factor $1/\sqrt{N}$ and the gain in terms of power is then N as compared to a single antenna. In other directions, the contributions from the different antennas can add destructively and may even completely cancel each other so that the amplitude is zero. A receiving antenna converts the incident wave into a signal, whose amplitude therefore depends on its position as illustrated in Fig. 4.1.

The maximum gain can be increased by having more antennas in the array. However, for cellular network, it is typically of interest to have a high antenna gain in all the directions where there are users, and this is enabled by a beamformer that adjusts the amplitude and delay of the signal transmitted from each antenna. Compared to the case when exactly the same signal is transmitted from all antennas, the direction of the maximum gain can thereby be changed so that it is obtained in a desired direction rather than right in front of the antenna array (see the example in Fig. 4.2).

In the present chapter, the opportunities offered by an array of antennas will be demonstrated, primarily by deriving the gain as a function of direction. The case with an antenna array used for transmission of a narrowband bandpass signal to a single receiving antenna is considered and rather than using formulations based on the electric fields and deriving radiation intensities, the radio channel model in Section 3.6.2 is used for the free-space single-path case in Section 3.6.2.6. The reason for taking the approach based on the channel model is to prepare for the MIMO OFDM channel model in Section 5.2 which is an extension of the model presented in the present chapter. The MIMO channel model will include multiple antennas at both the transmitting and receiving

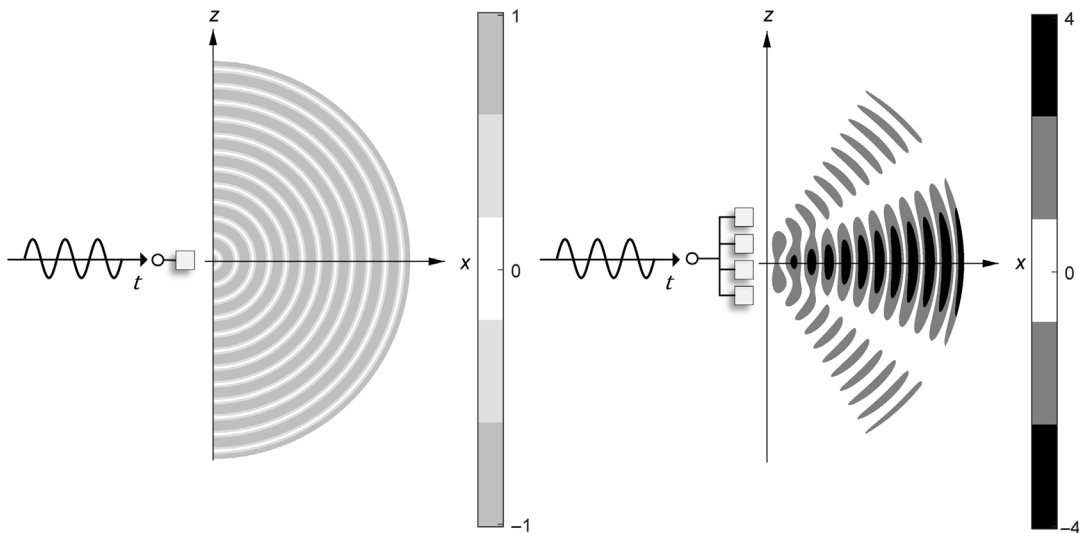


FIGURE 4.1

Illustration of the signal amplitude for different receiver positions in the xz -plane for a fixed time when a sinusoid is transmitted using one antenna (left) or four antennas (right). The amplitude of the signal is given by the bar legends.

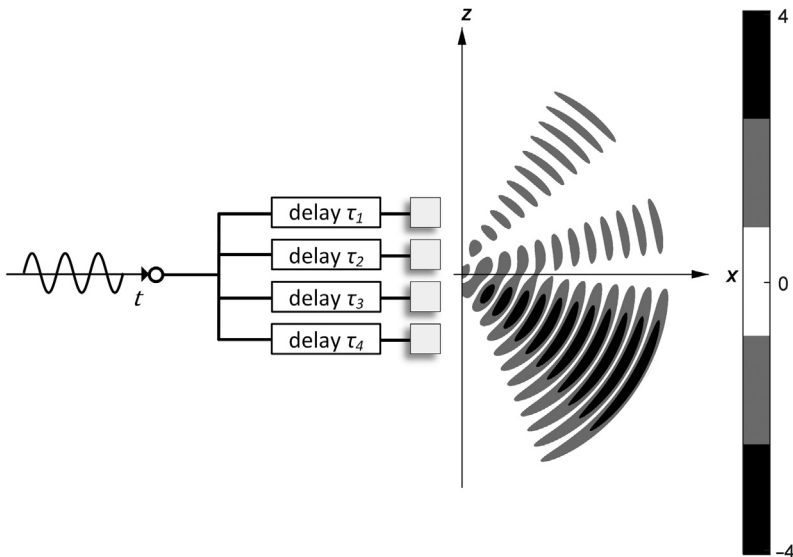


FIGURE 4.2

By transmitting the same signal from all antennas with appropriate delays, $\{\tau_k\}$, the directions where the signals add constructively can be controlled.

sides for the case with wideband OFDM-based transmission and serve as a basis for Chapter 6 on multiple antenna techniques.

Similar to Refs. [1,2], the starting point taken in Section 4.2 is the case with two identical transmitting antennas in free space. The signal received by an isotropic antenna in a certain direction is derived for the case that the same signal is transmitted from both antennas. As will be seen, the signal's amplitude is proportional to a product of the transmitting antennas' amplitude pattern and an array factor. Furthermore, some basic properties of the gain will be described and illustrated. Then, in Section 4.3, a more general antenna array with an arbitrary number of elements is considered, where *element* refers to an antenna in the array. The array response vector is introduced and related to the free-space single-path channel. Thereafter, it is shown that by also introducing a beamforming weight vector that represents the signals transmitted, the received signal's complex amplitude and consequently also the gain, is given by a product between the two vectors. The uniform linear array (ULA) is defined and it is shown that the maximum gain increases with the number of elements while the width of the main lobe decreases.

Classical beamforming, introduced in Section 4.4, allows changing the direction in which the maximum gain occurs by transmitting the same signal from all the elements, but with delays, or equivalently phase shifts chosen so that the signals add constructively in the desired direction. ULAs are then considered, and some remarks are made on element spacing as well as on so-called grating lobes. Some other forms of beamforming techniques are also illustrated to make the point that the properties of the gain pattern depend not only on the array but also on the beamformer used.

The UPA and the dual-polarized UPA are defined in [Section 4.5](#). These configurations represent commonly used special cases of the general array introduced in [Section 4.3](#) and some basic properties of the gain patterns are examined. With a UPA consisting of dual-polarized element pairs, not only the direction of the main lobe but also the polarization can be controlled.

[Section 4.6](#) introduces so-called arrays of subarrays. A dual-polarized UPA can be partitioned into subarrays and a benefit of this is that fewer radio chains are needed. At the same time, this constrains the set of beamforming weight vectors that can be applied to the antennas of the underlying array. For classical beamforming, the dependency between the subarray size and the range of angles with high gain is illustrated; the larger the subarray, the smaller the range of angles. This builds intuition for why different deployments call for different subarray sizes as will be illustrated in Sections 13.4 and 14.3.

Finally, in [Section 4.7](#), the key findings of the chapter are summarized.

4.2 ARRAYS WITH TWO ELEMENTS

Before addressing arrays with arbitrary many antennas, the case with two identical antennas transmitting the same signal is considered. If the signal transmitted is a sinusoid of a certain frequency, the antennas convert the signal to sinusoidal electromagnetic waves. A receiving antenna at a certain location will convert the sum of the two incident waves into a received signal. This is illustrated in [Fig. 4.3](#).

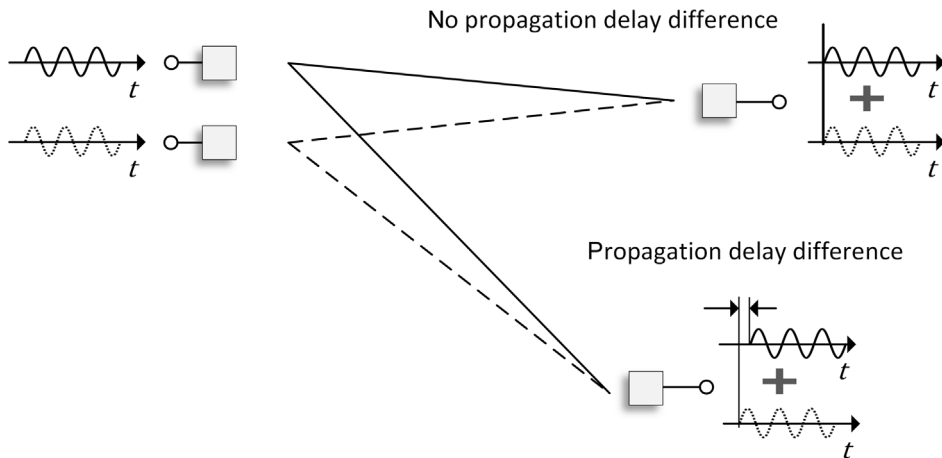


FIGURE 4.3

The received signal is a sum of the signals transmitted from the two antennas. The two signals may experience different propagation delays depending on the receiver's position.

The received signal's amplitude will depend on the difference in propagation delays for the signals transmitted from the two transmitting antennas which in turn depends on the direction from the transmitting antennas to the receiver. If the receiver is right in front of the two transmitting antennas so that the propagation delays are the same, then two signals will add constructively so that the amplitude is twice that of the signal received from a single antenna. If, however, the two signals have experienced different propagation delays, then the amplitude will depend on the time delay difference. In fact, the signals may completely cancel each other. For the case of a sinusoid signal, complete cancelation occurs if the delay difference equals half a period that corresponds to a propagation path length difference of half a wavelength.

From a received signal perspective, the array with two identical transmitting antennas appears as a single antenna with a (complex) amplitude pattern (see Section 3.3.4) that thus depends on the direction to the receiver. The amplitude of the received signal will also depend on the amplitude patterns of the individual transmitting antennas, which as mentioned above are referred to as *elements* in the context of the array. More specifically, the amplitude pattern for the array antenna can for the case with identical elements be expressed as a product of the element amplitude pattern and an array factor, which captures the summation of the signals from the individual elements. Note that the amplitude pattern also determines the gain pattern of the antenna array, that is, the power received as a function of direction relative to a single isotropic transmitting antenna.

Next, the amplitude pattern of the two-element array is derived and used to illustrate some properties of the gain pattern, such as a 3 dB increase in maximum gain as well as a narrower main lobe width relative to a single element.

4.2.1 ASSUMPTIONS

The transmitting and receiving antennas are in free space as depicted in Fig. 4.4. On the transmitting side, a vertical array with two identical elements placed along the z -axis with separation d is considered. The receiver antenna is placed at a distance R from the origin at a position determined by zenith and azimuth angles θ and φ in a right-handed spherical coordinate system (see also Appendix 1). The position of the receiver relative to the origin is given by the vector \mathbf{r} ,

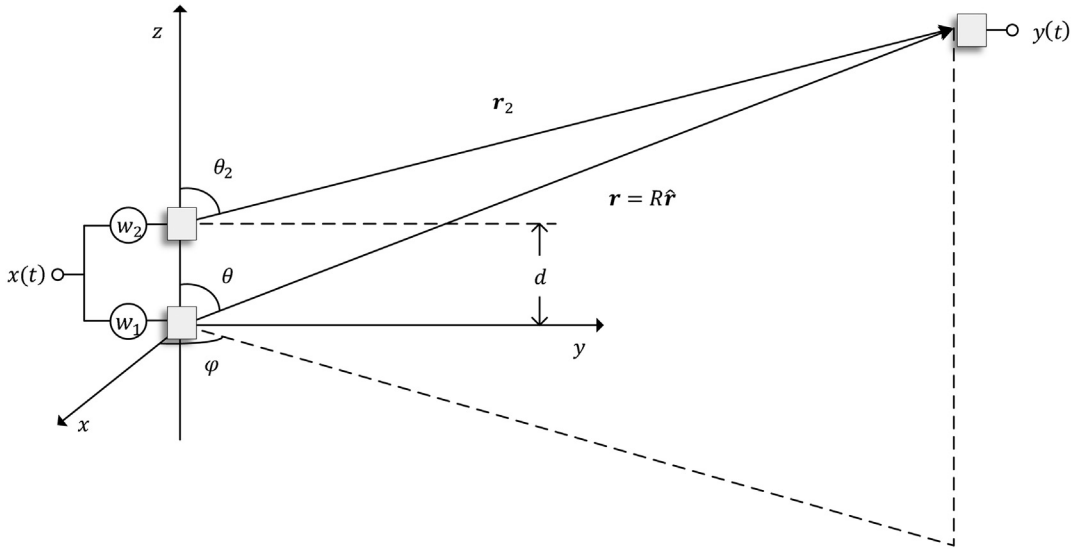
$$\mathbf{r} = R\hat{\mathbf{r}}, \quad (4.1)$$

where the spherical unit vector $\hat{\mathbf{r}}$ in Cartesian coordinates is described by

$$\hat{\mathbf{r}} = [\sin\theta\cos\varphi \quad \sin\theta\sin\varphi \quad \cos\theta]^T. \quad (4.2)$$

The first transmitting element is located at the origin and therefore \mathbf{r} also represents the propagation path from the first element to the receiving antenna. The propagation path from the second element to the receiving antenna is represented with the vector \mathbf{r}_2 . To isolate the impact of the transmitting elements, the receiver antenna is finally assumed to be isotropic, lossless and aligned in terms of polarization to the incident waves.

A key assumption that will be used in the derivation of the gain below is that the receiver is located at a large enough distance so that the propagation paths from the two transmitting elements, \mathbf{r} and \mathbf{r}_2 , appear (approximately) parallel (see also [1–3]).

**FIGURE 4.4**

A transmitting two-element vertical array with element separation d

The assumption is illustrated in Fig. 4.5, together with the vector \mathbf{d}_2 that represents the second element's position,

$$\mathbf{d}_2 = [0 \ 0 \ d]^T, \quad (4.3)$$

and the propagation path from the second element

$$\mathbf{r}_2 = R_2 \hat{\mathbf{r}},$$

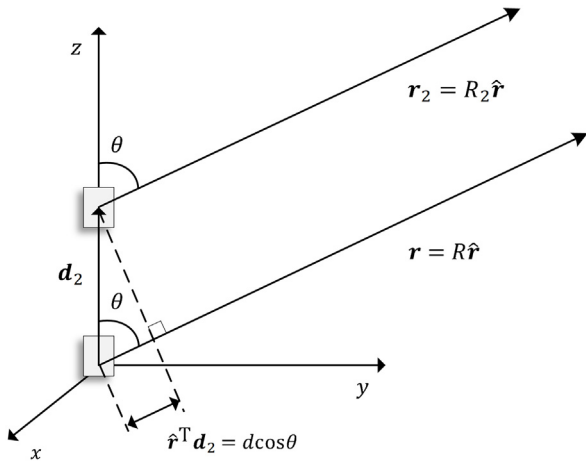
where R_2 denotes the corresponding path length. The propagation path length of the second element, R_2 , can be expressed as the projection of \mathbf{r}_2 onto $\hat{\mathbf{r}}$

$$R_2 = \hat{\mathbf{r}}^T \mathbf{r}_2 = \hat{\mathbf{r}}^T (\mathbf{r} - \mathbf{d}_2) = R - \hat{\mathbf{r}}^T \mathbf{d}_2 = R - d \cos \theta, \quad (4.4)$$

where the second equality follows from that the propagation path for the second element can be expressed as $\mathbf{r}_2 = \mathbf{r} - \mathbf{d}_2$. Since the paths \mathbf{r} and \mathbf{r}_2 are assumed parallel, the angular direction to the receiver is furthermore equal to θ for both elements. An interpretation of the approximation of parallel paths is that the waves incident on the receiver from the two transmitting elements can be seen (locally) as plane waves propagating in the same direction $\hat{\mathbf{r}}$ (see also the discussion of wave fronts in Section 3.2.2).

Some assumptions are also needed on the signals transmitted and received. More specifically, as shown in Fig. 4.4, the same signal is transmitted from both elements, and for a fair comparison to the case with a single element, the total transmit power is kept the same. This means in this case with two elements that each element uses half the power, and the signals transmitted are taken as

$$x_1(t) = w_1 x(t), \quad (4.5)$$

**FIGURE 4.5**

The distance to the receiver is large so that the two paths to the receiver (not shown in the figure), \mathbf{r} and \mathbf{r}_2 , appear parallel.

$$x_2(t) = w_2 x(t), \quad (4.6)$$

with amplitude weights chosen as

$$w_1 = w_2 = 1/\sqrt{2}. \quad (4.7)$$

The transmitted signal $x(t)$ as well as the received signal, $y(t)$, are complex-valued low-pass basebands equivalents [4,5], and the actual signals at radio frequency are narrowband signals given by

$$x_{\text{RF}}(t) = \text{Re}\{x(t)e^{j2\pi f_c t}\}, \quad (4.8)$$

$$y_{\text{RF}}(t) = \text{Re}\{y(t)e^{j2\pi f_c t}\}, \quad (4.9)$$

where f_c is the carrier frequency (see also Section 3.6.2.1 and Fig. 3.27). The special case that the transmitted radio frequency signal is a single-frequency sinusoid means that

$$x(t) = X \rightarrow x_{\text{RF}}(t) = |X| \cos(2\pi f_c t + \arg\{X\}), \quad (4.10)$$

and the magnitude and argument of X thus represent the amplitude and phase of the sinusoid.

4.2.2 RECEIVED SIGNAL IN A FREE-SPACE CHANNEL

Due to the superposition principle (see Section 3.2.4), the received signal $y(t)$ will be a sum of the contributions from the two transmit elements. To determine the contribution from each transmitting element, the multipath propagation model in Section 3.6.2 is used for the special case with a single path to represent free-space propagation. Omitting for simplicity any thermal noise, the received

signal can then be written as

$$y(t) = h_1 x_1(t - \tau_1) + h_2 x_2(t - \tau_2) \quad (4.11)$$

where h_n and τ_n represent the complex amplitude and propagation delay for the propagation path associated with transmit element n . More specifically, it can be shown using the definition of the antenna radiation pattern in (3.30) and the free-space radio channel model defined in Section 3.6.2.6 that the complex amplitudes h_n can be expressed as

$$h_n = \alpha e^{-j2\pi f_c \tau_n} g_r(\theta_r, \varphi_r) g_t(\theta, \varphi) \chi. \quad (4.12)$$

Here, α represents the path loss between isotropic lossless antennas, θ_r and φ_r represent the direction at the receiver, $g_r(\theta, \varphi)$ and $g_t(\theta, \varphi)$ are the (complex) amplitude patterns for the receiver antenna and the transmitting elements, respectively. The term χ captures the alignment between the polarization of the receiver antenna, $\hat{\psi}_r(\theta_r, \varphi_r)$, and the polarization of the transmitting elements, $\hat{\psi}_t(\theta, \varphi)$ (see also Section 3.4.2).

As a side note, for the case that the propagation paths r and r_2 are not parallel, (4.11) still holds but the complex amplitude gains in (4.12) would need to be modified since the angles $\theta_r, \varphi_r, \theta$, and φ are different for the two elements. Another implicit and reasonable assumption is that the distance between the two elements, d , is much smaller than the propagation path lengths so that the path loss in terms of α is the same for both elements.

To demonstrate the gain of using two transmit elements, the expression in (4.12) is next further simplified using the assumption that the receiver antenna is isotropic, lossless and aligned in terms of polarization so that

$$g_r(\theta_r, \varphi_r) = 1, \quad (4.13)$$

$$\chi = 1. \quad (4.14)$$

By combining the four last equations, together with the definitions of the transmitted signals in (4.5) and (4.6) the received signal becomes

$$y(t) = \alpha e^{-j2\pi f_c \tau_1} g(\theta, \varphi) w_1 x(t - \tau_1) + \alpha e^{-j2\pi f_c \tau_2} g(\theta, \varphi) w_2 x(t - \tau_2), \quad (4.15)$$

where $g(\theta, \varphi) = g_t(\theta, \varphi)$ is the complex amplitude pattern for a transmitting element. Thus, the received signal is as expected a sum of two versions of the transmitted signal with different propagation delays, and the factor $e^{-j2\pi f_c \tau_n}$ represents the phase shift caused by the propagation delay of element n . The propagation delays can in turn using (4.4) be expressed as

$$\tau_1 = \frac{R}{c}, \quad (4.16)$$

$$\tau_2 = \frac{R_2}{c} = \frac{R}{c} - \frac{d \cos \theta}{c} = \tau_1 - \frac{d \cos \theta}{c}, \quad (4.17)$$

where c is the wave propagation speed.

In the next section, the last three expressions will be combined to establish a gain relation between the transmitted and received signals as a function of direction. This is possible since the propagation delay difference does depend on θ and φ in the general case, and on θ in the particular case.

4.2.3 GAIN AND ARRAY FACTOR

The expression for the received signal is further refined using properties of the transmitted signal. For the case that the signal transmitted is a sinusoid as defined in (4.10), also the received signal, as obtained by substituting $x(t) = X$ in (4.15), is a sinusoid at radio frequency,

$$x(t) = X \rightarrow y(t) = Y \leftrightarrow y_{RF}(t) = |Y|\cos(2\pi f_c t + \arg\{Y\}). \quad (4.18)$$

Next, the expressions for propagation delays in (4.16), and (4.17), and the fact that $x(t)$ corresponds to a sinusoid at radio frequency is again used in (4.15). Then, by defining the array factor, $\text{AF}(\theta, \varphi)$, as

$$\text{AF}(\theta, \varphi) = w_1 + w_2 e^{jkd\cos\theta}, \quad (4.19)$$

using the relation between carrier frequency f_c , wave propagation speed c , and the magnitude of the wave vector defined in Section 3.2,

$$k = \|\mathbf{k}\| = \frac{2\pi}{\lambda} = \frac{2\pi f_c}{c}, \quad (4.20)$$

the amplitude and phase of the received sinusoid can be expressed as

$$Y = \alpha e^{-j2\pi f_c \tau_1} \underbrace{\text{AF}(\theta, \varphi) g(\theta, \varphi)}_{= g_{AA}(\theta, \varphi)} X \quad (4.21)$$

As can be seen from (4.21), the received signal amplitude, $|Y|$ depends on the product of the elements' amplitude pattern as well as the array factor which thus describes how the contributions from the two elements sum up. In fact, by comparing (4.21) with using only the first element ($w_1 = 1, w_2 = 0 \leftrightarrow \text{AF}(\theta, \varphi) = 1$), the received signal appears to be transmitted from a single antenna with (complex) amplitude pattern

$$g_{AA}(\theta, \varphi) = \text{AF}(\theta, \varphi) g(\theta, \varphi), \quad (4.22)$$

rather than from an antenna with amplitude pattern $g(\theta, \varphi)$. This explains why an antenna array may also be referred to as an antenna. The amplitude pattern for the array transmission, $g_{AA}(\theta, \varphi)$, will just as any other amplitude pattern characterize radiation properties such as its gain pattern which relates to the transmitted and received power rather than amplitude. By squaring the magnitude of both sides of (4.21), the relation between transmitted and received power is

$$|Y|^2 = \alpha^2 G_{AA}(\theta, \varphi) |X|^2,$$

where the gain as a function of direction has been defined as

$$G_{AA}(\theta, \varphi) = |g_{AA}(\theta, \varphi)|^2 = |\text{AF}(\theta, \varphi)|^2 G(\theta, \varphi). \quad (4.23)$$

Here, $G(\theta, \varphi) = |g(\theta, \varphi)|^2$ is the (power) gain pattern for one element in the array. Thus, it is assumed that the complex amplitude pattern $g(\theta, \varphi)$ is scaled so that $G(\theta, \varphi)$ is the (antenna) gain as

a function of direction relative to an isotropic lossless antenna for one element (see also Section 3.3.7.4). Before examining and illustrating the gain pattern defined by (4.23), the following is noted:

- The amplitude pattern in (4.22) can be expressed as a product of the array factor and the element pattern. This will hold also for the larger arrays considered in later parts of the chapter, including both uniform linear and UPAs as well as cases with beamforming;
- For the gain pattern in (4.23), the factor $|\text{AF}(\theta, \varphi)|^2$ can be recognized as the gain pattern for an array of isotropic elements in terms of received power relative to a single isotropic antenna under free-space propagation conditions. This gain will be sometimes be referred to as the (*free-space*) *array gain*. The gain pattern for the antenna array in (4.23) is thus the product of this array gain and the element gain patterns.

Having made these observations, some properties of the gain pattern are explored and illustrated in Section 4.2.4 before showing in Section 4.2.5 that the findings apply not only to single-frequency signals but also to narrowband signals.

4.2.4 PROPERTIES OF THE GAIN

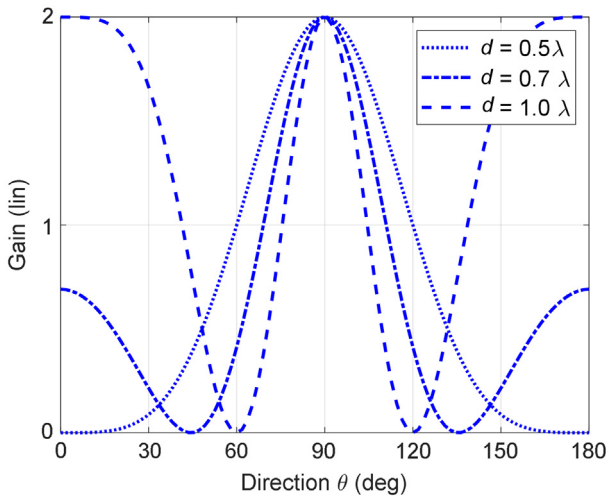
To further understand the properties of the (power) gain defined in (4.23), Euler's formula is used together with the assumption on transmitting the same signal from both elements. Combining (4.7) and (4.19) gives

$$|\text{AF}(\theta, \varphi)|^2 = 2 \left| \cos\left(\frac{k}{2} d \cos\theta\right) \right|^2. \quad (4.24)$$

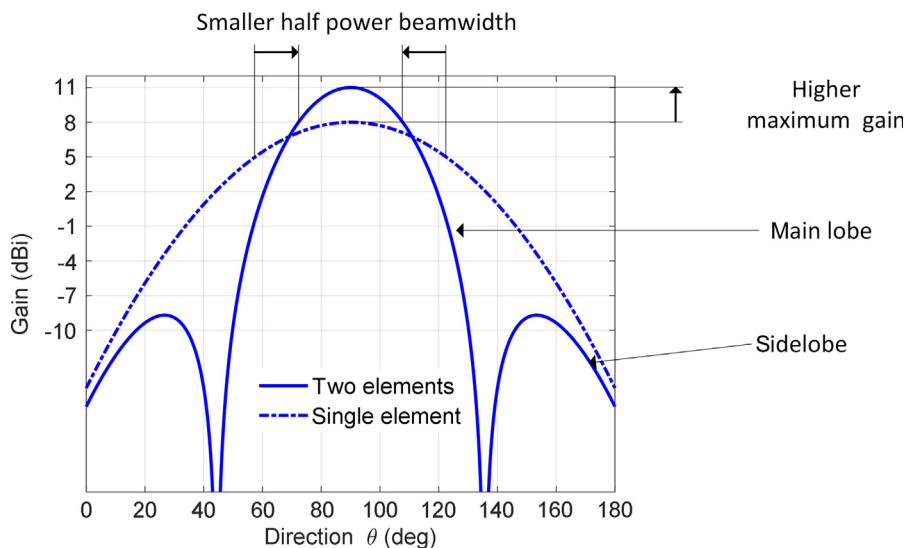
As discussed in Section 4.2.3, this can be recognized as the free-space array gain pattern, and in Fig. 4.6 this gain is illustrated as a function of direction θ for some different element separations d . From the expression in (4.24), it is noted that

- The free-space array gain has its maximum value two, $|\text{AF}(\theta, \varphi)|^2 = 2$, for angles θ that satisfy $d \cos\theta = 0, \pm \lambda, \pm 2\lambda, \dots$. For such angles, the received power is twice as high, or 3 dB higher, as compared to the case with a single element using the same total transmit power since the signals received combine constructively. From (4.4), $d \cos\theta$ can be recognized as the propagation path length difference between the two antennas, and hence constructive addition occurs when the path length difference equals a multiple of the wavelength;
- The free-space array gain attains its minimum value, $|\text{AF}(\theta, \varphi)|^2 = 0$ for angles such that $d \cos\theta = \pm \frac{\lambda}{2}, \pm \frac{3\lambda}{2}, \dots$. This means that when the propagation path length difference is an odd multiple of half the wavelength, the signals from the two antennas will cancel each other. For the case with $d = 0.7\lambda$, there will be zeros for $\theta \approx 90^\circ \pm 45^\circ$.

Thus, the signals from the two elements can add constructively in certain directions but also cancel out in other directions as stated in the introduction. However, the total gain in a certain direction depends not only on the array gain but also on the gain of the elements in the array in the same direction according to (4.23). In Fig. 4.7, gain patterns are illustrated, both for a single element of the array, and for a two-element array consisting of two such elements. The element pattern defined in [6] with 65-degree half-power beamwidth and 8 dBi gain is used, and the separation

**FIGURE 4.6**

Gain on linear scale of using a two-element array relative, a single element for the case with isotropic elements.

**FIGURE 4.7**

Gain as function of direction θ for $\varphi = 0^\circ$ for a single element and an array with two such elements separated by 0.7λ . The element gain model in [6] is used and the elements are oriented so that the maximum gain occurs for $\theta = 90^\circ, \varphi = 0^\circ$.

between the element is $d = 0.7\lambda$. The impact of the element separation is elaborated on further in [Section 4.4.2.1](#).

As can be seen, the maximum gain, which occurs for $\theta = 90^\circ$, is 3 dB higher compared to a single element aligned to have maximum gain in this direction.

Also, the half-power beamwidth of the main lobe, which is the range of angles for which the gain is within 3 dB of its maximum value, is smaller for the array as compared to the single-element case. Thus, the higher maximum gain comes at the cost of a narrower main lobe. This stems from the fact that the gain pattern is a product of the array gain and the element gain pattern. The gain pattern then typically has a beamwidth which is at least as narrow as the narrowest one of the two, in this case the array gain. Finally, for the chosen element separation $d = 0.7\lambda$, the array factor is zero for $\theta = 90^\circ \pm 45^\circ$ and the same holds for the total gain and this explains why there in addition to the main lobe also are sidelobes.

To complement the gain patterns given in [Figs. 4.6](#) and [4.7](#), which illustrated only the gain as a function of zenith angle θ , the dependency on both the zenith angle and the azimuth angle φ is illustrated on a logarithmic scale using spherical coordinates in [Fig. 4.8](#). For comparison, the case with a two-element horizontal array is also included. The difference as compared to the vertical array is the position of the second element which corresponds to replacing [\(4.3\)](#) with $\mathbf{d}_2 = [0 \ d \ 0]^T$. The same spacing $d = 0.7\lambda$ is used for both the horizontal and vertical arrays.

Both the vertical and horizontal arrays will have 3 dB higher maximum gain right along the x -axis as compared to the single-element case. The difference between the two patterns is that for the

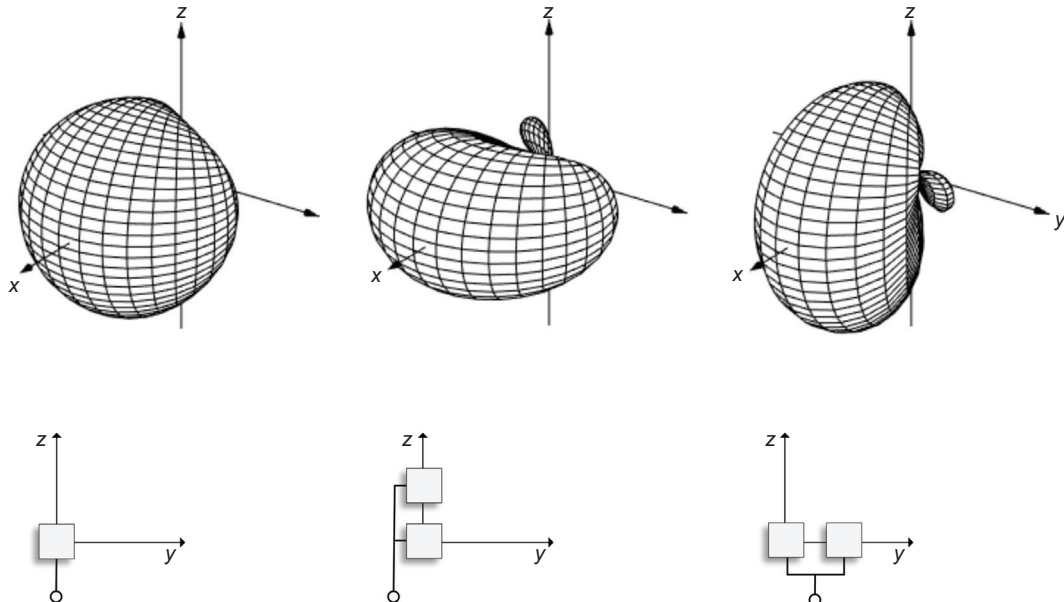


FIGURE 4.8

Illustration of gain in different directions for a single element (left), a vertical array with two elements (center) and a horizontal array with two elements (right). The element gain model in [\[6\]](#) is used in all three cases.

vertical array, the gain depends on the angle to the z -axis whereas it depends on the angle to y -axis for the horizontal array. The vertical array has a smaller main lobe width in the plane $\varphi = 0^\circ$ whereas the horizontal array has a smaller main lobe width in the horizontal plane $\theta = 90^\circ$.

To sum up, properties of the gain, for a two-element vertical array, have been considered. It was demonstrated that the gain can be increased with 3 dB while the main lobe width in the vertical plane was reduced. The same applies for a horizontal array except that the main lobe width in the horizontal plane is reduced.

4.2.5 EXTENSION TO NARROWBAND SIGNALS

The derivation of the gain is now extended also to narrowband signals. This essentially means that the assumption (4.18) is not used. Instead the key approximation done is

$$x(t - \tau_2) \approx x(t - \tau_1). \quad (4.25)$$

Such an approximation will be accurate for the case that the propagation delay difference $\Delta\tau = \tau_2 - \tau_1$ is small. Small in this context needs to be related to how fast the (baseband) signal $x(t)$ changes with time and as long as $B\Delta\tau \ll 1$, where B is the bandwidth of the signal, then (4.25) is a commonly used approximation in the field of array signal processing [7] (see also Section 3.6.2.5).

Eq. (4.25) may at first appear a bit unexpected since the propagation delay difference should give rise to a phase shift that is not visible in the equation. The reason for this is that the phase shift caused by the propagation delay is part of the channel coefficient in (4.15).

By using the relations (4.16), (4.17), and (4.25) in (4.15), the received signal can be expressed as

$$y(t) = \alpha e^{-j2\pi f_c \tau_1} \underbrace{\text{AF}(\theta, \varphi) g(\theta, \varphi)}_{g_{AA}(\theta, \varphi)} x(t - \tau_1) \quad (4.26)$$

From a receiver perspective, just as in the case with a single-frequency sinusoid, the signal appears as being transmitted from an antenna with amplitude pattern $g_{AA}(\theta, \varphi)$, which coincides with the definition in (4.22).

This means that the results derived in the previous subsections are valid not only for sinusoidal signals but to a wider class of signals. It should though be remembered that the delay difference depends on the element separation d (see (4.16) and (4.17)), and this means that (4.25) becomes inaccurate when the element separation and/or the bandwidth of the signal become too large. In that case, the signal can be partitioned into sub-bands, for example, sets of adjacent subcarriers in the case with OFDM as described in Chapter 5 with bandwidths small enough for the approximation to hold.

4.3 UNIFORM LINEAR ARRAYS WITH MORE THAN TWO ELEMENTS

The case with two transmitting elements was considered in Section 4.2. Attention is now shifted to the case with $N > 2$ transmitting elements at arbitrary locations in the same free-space propagation

scenario. The major difference as compared to the case with two elements is that the received signal is a sum of N versions of the transmitted signal.

To determine the gain as a function of direction for the array, a so-called *array response vector* will be defined. The array response vector includes the impact of the N elements' amplitude patterns and propagation delay differences, all depending on the direction of the receiver. By introducing a weight vector to represent the signal versions transmitted from all the elements, the complex amplitude for transmission with the array can be expressed as a product of the two defined vectors. The array response vector can also under certain assumptions be interpreted as a normalized free-space multiple-input-single-output (MISO) channel for transmission of a narrowband signal, and later in Section 5.3.2, the MIMO OFDM channel model will be formulated based on it.

The special but common case with a ULA is considered. For a ULA, the array is uniform in the sense that the separation between any two adjacent elements is the same and further all elements have the same amplitude pattern. The same signal is transmitted from all the elements, and at broadside, in the direction perpendicular to the array, the (power) gain as compared to transmission from a single element is N , stemming from coherent addition of contributions from all the N elements while keeping the total transmitted power the same as for the single-element case. However, as will be shown, the main lobe beamwidth scales approximately with the inverse of the length of the array, that is, as $\lambda/(dN)$, for an element separation d and wavelength λ . As a side note, it is observed that there are also nulls in the radiation pattern, indicating the possibility, not only to increase the gain in certain directions but also to reduce the gain in other directions.

4.3.1 ASSUMPTIONS

A free-space propagation scenario is considered, and the assumptions done are essentially the same as for the case with two elements described in [Section 4.2.1](#), with the following differences (see also [Fig. 4.9](#)):

- The array has N identical elements and the positions of the elements are described by the vectors

$$\mathbf{d}_n = [d_{x,n} \quad d_{y,n} \quad d_{z,n}]^T, n = 1, \dots, N, \quad (4.27)$$

relative to a common reference point in origin $[0 \quad 0 \quad 0]^T$.

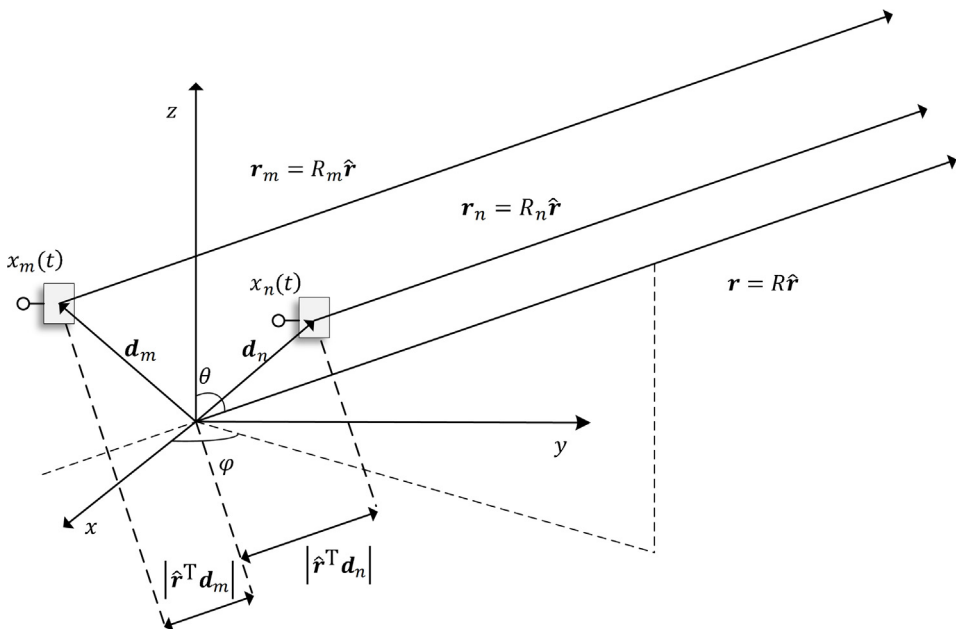
- The propagation path between element n and a receiving antenna is denoted \mathbf{r}_n and the distance to the receiver is large so that all propagation paths appear parallel

$$\mathbf{r}_n = R_n \hat{\mathbf{r}}, n = 1, \dots, N. \quad (4.28)$$

Here, $\hat{\mathbf{r}}$ defined in [\(4.2\)](#) points in the direction from the reference point to the receiver and R_n is the length of the corresponding propagation path. Considering [\(4.4\)](#), the path length can be expressed as

$$R_n = R - \hat{\mathbf{r}}^T \mathbf{d}_n, \quad (4.29)$$

where R is the path length from the reference point for the element positions and $\hat{\mathbf{r}}^T \mathbf{d}_n$ is the projection of \mathbf{d}_n onto $\hat{\mathbf{r}}$.

**FIGURE 4.9**

The distance to the receiver is large so that two paths r_n and r_m to the receiver (not shown in the figure) from two elements with positions d_n and d_m appear parallel.

- The signal transmitted from element n is taken as

$$x_n(t) = w_n x(t), \quad n = 1, \dots, N. \quad (4.30)$$

For the case that the same signal is transmitted from all the elements the weights are chosen as

$$w_n = 1/\sqrt{N}, \quad n = 1, \dots, N, \quad (4.31)$$

to allow a fair comparison between different array sizes that use the same amount of total power.

- The signal $x(t)$ represents a narrowband signal with bandwidth small enough so that

$$x(t - \tau_n) \approx x(t - \tau), \quad n = 1, \dots, N, \quad (4.32)$$

where τ and τ_n represent the propagation delay from the reference point and element n , respectively, to the receiving antenna,

$$\tau = \frac{R}{c}, \quad (4.33)$$

$$\tau_n = \frac{R_n}{c}. \quad (4.34)$$

The approximation in (4.32) holds obviously for a single-frequency sinusoid as defined in (4.10), and is also, as discussed in Section 4.2.5, applicable for narrowband signals with bandwidth B such that the propagation delay differences, which can be related to the element positions using (4.29),

$$\Delta\tau_n = \tau_n - \tau = -\frac{\mathbf{r}^T \mathbf{d}_n}{c}, \quad n = 1, \dots, N, \quad (4.35)$$

satisfy $B\Delta\tau_n \ll 1$. Recall from the discussion in Section 4.2.5 that the approximation may become inaccurate if the array or the bandwidth becomes too large.

This set of assumptions is next used to define an array response vector and a beamforming weight vector that leads to a compact formulation of the received signal.

4.3.2 ARRAY RESPONSE VECTOR AND BEAMFORMING WEIGHT VECTOR

For the case with two elements, it was found in Section 4.2.3 that the received signal appears to be transmitted from a single antenna with (complex) amplitude pattern determined as a product of an array factor and the element amplitude pattern as in (4.22) and this holds also for the case with N elements. The amplitude pattern can however also be expressed as a product, between an *array response vector* and a *beamforming weight vector*, and next these two vectors are defined, discussed and related to the gain.

The starting point is to generalize (4.15) to the case with N signals. By using the narrowband assumption in (4.32) for the relative propagation delays in (4.35), it follows that the generalized expression (4.15) can be written as

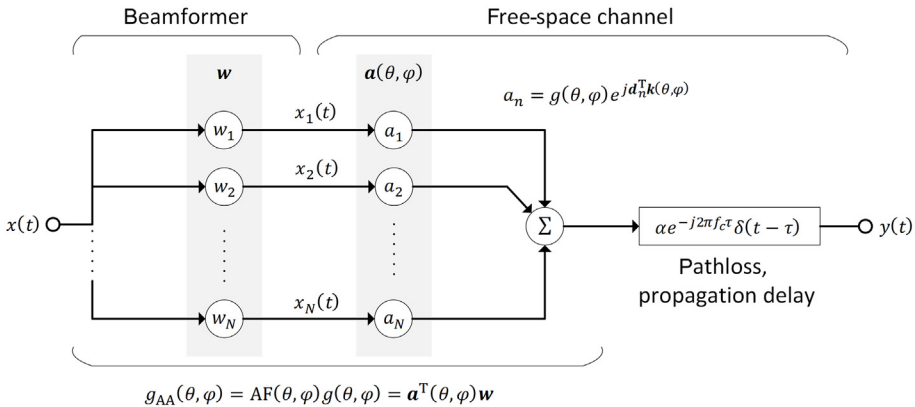
$$y(t) = \sum_{n=1}^N \alpha e^{-j2\pi f_c \tau} e^{-j2\pi f_c \Delta\tau_n} w_n g(\theta, \varphi) x(t - \tau). \quad (4.36)$$

The relation between the transmitted and received signal is illustrated in Fig. 4.10. As can be seen, a beamformer generates weighted versions of the signal $x(t)$ for the different antennas as described by (4.30). The weights $\{w_n\}$ are collected in a vector with N elements, a *beamforming weight vector*

$$\mathbf{w} = [w_1 \quad w_2 \quad \cdots \quad w_N]^T. \quad (4.37)$$

For now, it is assumed that the same signal is transmitted from all the elements, and the corresponding weights w_n are defined in (4.31). Other choices of (complex-valued) weights will be discussed in Section 4.4.

As shown in Fig. 4.10, there is also effectively a MISO channel between the N transmitting elements and the receiver. All the elements share the same path loss and a common propagation delay as given by (4.33). However, since the elements are at different positions the corresponding received signals experience different propagation delays, which depends on the direction, and this part of the channel may be represented by the array response vector. The elements' complex amplitude patterns depend also on the direction and may, in the general case, differ between the elements. For these reasons they are, together with the phase shift caused by the propagation delay difference relative to the common propagation delay, collected into the array response vector.


FIGURE 4.10

Relation between transmitted signal $x(t)$ and received signal $y(t)$.

The array response vector can therefore be seen as a normalized free-space MISO channel between the transmitted signals $\{x_n(t), n = 1, \dots, N\}$ and the signal received by the isotropic polarization-aligned antenna $y(t)$. The normalization implies that it neither includes the impact of the propagation delay τ between the reference point of the array and the receiver, nor the path loss as represented with α .

Since all the elements are assumed to have the same complex amplitude pattern, $g(\theta, \varphi)$, the *array response vector* becomes

$$\mathbf{a}(\theta, \varphi) = g(\theta, \varphi) \begin{bmatrix} e^{j\mathbf{d}_1^T \mathbf{k}(\theta, \varphi)} & e^{j\mathbf{d}_2^T \mathbf{k}(\theta, \varphi)} & \dots & e^{j\mathbf{d}_N^T \mathbf{k}(\theta, \varphi)} \end{bmatrix}^T, \quad (4.38)$$

where the *wave vector* $\mathbf{k}(\theta, \varphi)$ is a scaled version of $\hat{\mathbf{r}}$ defined in (4.2),

$$\mathbf{k}(\theta, \varphi) = \frac{2\pi}{\lambda} \hat{\mathbf{r}} = \frac{2\pi}{\lambda} [\sin\theta \cos\varphi \quad \sin\theta \sin\varphi \quad \cos\theta]^T. \quad (4.39)$$

By combining (4.35), (4.20), and (4.39) in sequence, the phase shift caused by the delay difference is related to the phase shifts of the array response vector in (4.38) as follows

$$e^{-j2\pi f_c \Delta\tau_n} = e^{j2\pi f_c \frac{\hat{\mathbf{r}}^T \mathbf{d}_n}{c}} = e^{j\frac{2\pi}{\lambda} \hat{\mathbf{r}}^T \mathbf{d}_n} = e^{j\mathbf{k}^T(\theta, \varphi) \mathbf{d}_n} = e^{j\mathbf{d}_n^T \mathbf{k}(\theta, \varphi)}, \quad (4.40)$$

for $n = 1, \dots, N$. The received signal in (4.36) can then be written on the form

$$y(t) = \alpha e^{-j2\pi f_c \tau} g_{AA}(\theta, \varphi) x(t - \tau), \quad (4.41)$$

where the amplitude pattern $g_{AA}(\theta, \varphi)$ can be expressed as a product of the beamforming weight vector and the array response vector

$$g_{AA}(\theta, \varphi) = \mathbf{a}^T(\theta, \varphi) \mathbf{w}. \quad (4.42)$$

The combination of the beamformer and the array response vector thus appears as an antenna with amplitude pattern $g_{AA}(\theta, \varphi)$. This is illustrated in Fig. 4.10 together with the relations to the

beamformer and the array response vector. The corresponding gain pattern in terms of received power relative to an isotropic lossless antenna can be expressed by combining (4.23) and (4.42) as

$$G_{AA}(\theta, \varphi) = |g_{AA}(\theta, \varphi)|^2 = |\mathbf{a}^T(\theta, \varphi)\mathbf{w}|^2. \quad (4.43)$$

This gain pattern is sometimes also referred to as *beam gain pattern* or *beam pattern*. Given an array response vector as a function of direction for a particular array in terms of element pattern and positions, such a beam pattern can thus be determined for a beamformer using (4.43).

Previously, in (4.22) and (4.26), it was also found that the amplitude pattern in (4.42) could be expressed as a product of an array factor and the element pattern. As all elements are assumed to be the same, this holds also for the case with N elements and the array factor can be written as

$$AF(\theta, \varphi) = \sum_{n=1}^N w_n e^{j\mathbf{d}_n^T \mathbf{k}(\theta, \varphi)}, \quad (4.44)$$

so that (4.22), repeated here for convenience, can be used to also express the amplitude pattern as

$$g_{AA}(\theta, \varphi) = AF(\theta, \varphi)g(\theta, \varphi). \quad (4.45)$$

Thus, for the case that all elements of the array are the same, the amplitude pattern can be expressed on two different but equivalent forms as given by (4.42) and (4.45). For the case that the elements are significantly different, (4.45) does not apply. In that case the array response vector needs to be modified and (4.42) can be used to determine the amplitude pattern.

In the next section some properties of the gain pattern $G_{AA}(\theta, \varphi)$ are illustrated for the special but common case of ULAs.

4.3.3 UNIFORM LINEAR ARRAYS

A ULA is a special but very common antenna array used in practice. Here the array is uniform in the sense that the separation between any two adjacent elements is the same and all elements have the same amplitude pattern. Both vertical and horizontal array arrangements are possible (see Fig. 4.11). Vertical arrangements, also referred to as column antennas, of dual-polarized element pairs introduced in Section 4.5.2, are by far the most common structure for classical base stations antennas.

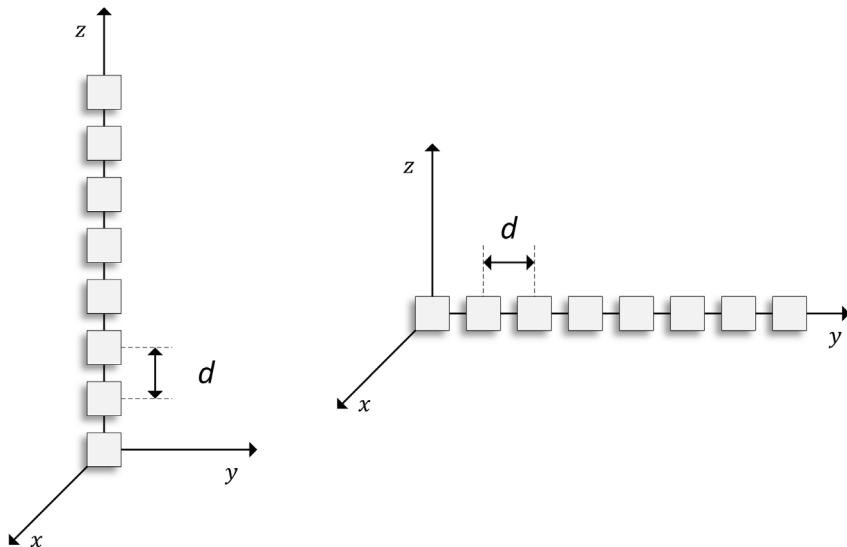
For analysis purposes the following characteristics are assumed:

- The positions of the elements \mathbf{d}_n are taken along the positive z -axis for a vertical array and along the positive y -axis for a horizontal array

$$\mathbf{d}_n = \begin{cases} (n-1)[0 \ 0 \ d]^T & \text{vertical array (along } z\text{-axis)} \\ (n-1)[0 \ d \ 0]^T & \text{horizontal array (along } y\text{-axis)} \end{cases}. \quad (4.46)$$

- All elements have the same complex amplitude pattern $g(\theta, \varphi)$ oriented so that the maximum (magnitude) occurs in the direction of the x -axis, $\theta = 90^\circ$, $\varphi = 0^\circ$.

The assumption that all elements have the same pattern is an approximation. In antenna arrays, the separation between adjacent elements is typically rather small, less than a wavelength as discussed in Section 4.4.2.1, and the elements will interact with each other. This interaction is referred

**FIGURE 4.11**

Examples with eight elements: vertical (left) and horizontal (right) uniform linear arrays.

to as mutual coupling [1,3] (see also Section 12.3.7). One consequence of this is that the gain patterns for the elements are different when they are used in an array as compared to when they are used in isolation. A common approach in analysis, design, and evaluations is therefore to incorporate the impact of mutual coupling by using a so-called embedded pattern rather than the pattern for the element in isolation, and in line with this all elements are assumed to have the same pattern.

4.3.3.1 Basic gain patterns

To explore some basic properties of a ULA, the gain as a function of the direction (θ, φ) will be considered for the case that the same signal is transmitted from all antennas. The approach taken is to first use the expression for the (complex) amplitude pattern in (4.42) or (4.45) and then determine the gain as the squared magnitude of it as given by (4.43). The array response vector for the ULA can be determined by combining (4.38) and (4.46) and the beamforming weight vector is chosen as

$$\mathbf{w} = [w_1 \quad w_2 \quad \cdots \quad w_N]^T = \frac{1}{\sqrt{N}} \underbrace{[1 \quad 1 \quad \cdots \quad 1]^T}_{N \text{ ones}}, \quad (4.47)$$

to represent the case that the same signal is transmitted from all antennas as defined in (4.31).

The gain patterns for vertical and horizontal arrays with different number of elements are illustrated using a logarithmic scale in Figs. 4.12 and 4.13, respectively. In both cases, the element amplitude pattern defined in [6] with 65-degree half-power beamwidth and 8 dBi gain is used, and the separation between the elements is $d = 0.7\lambda$. Similar to the case with two elements, increasing the number of elements in either the vertical or horizontal dimension reduces the width of the main

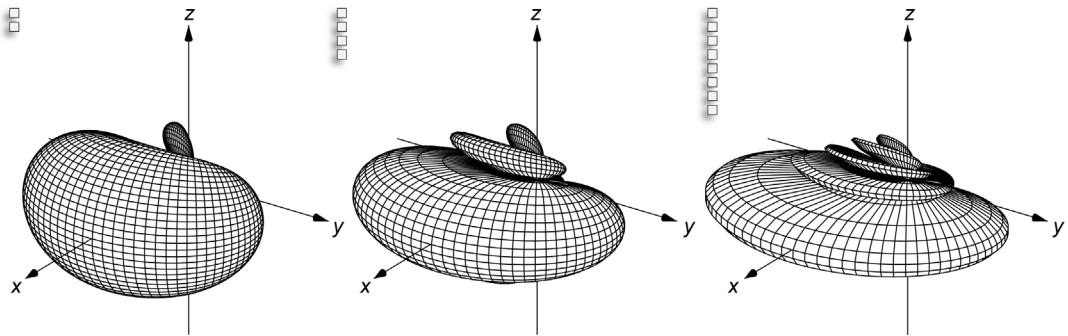
**FIGURE 4.12**

Illustration of gain pattern for vertical arrays with two, four, and eight elements.

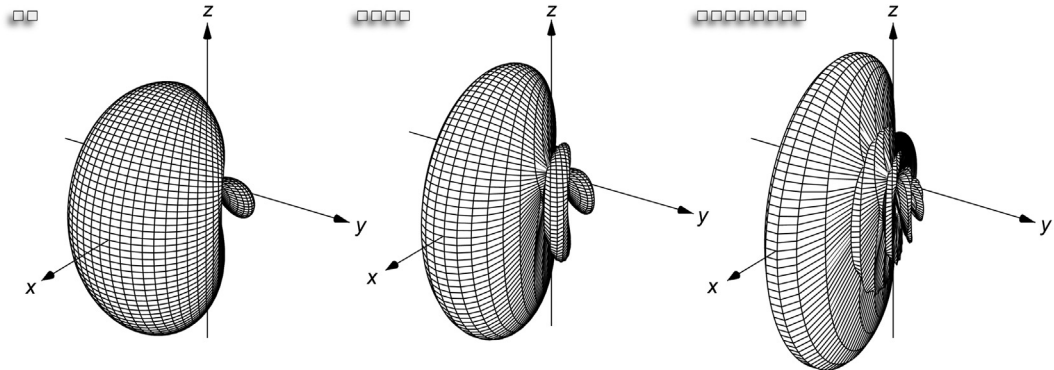
**FIGURE 4.13**

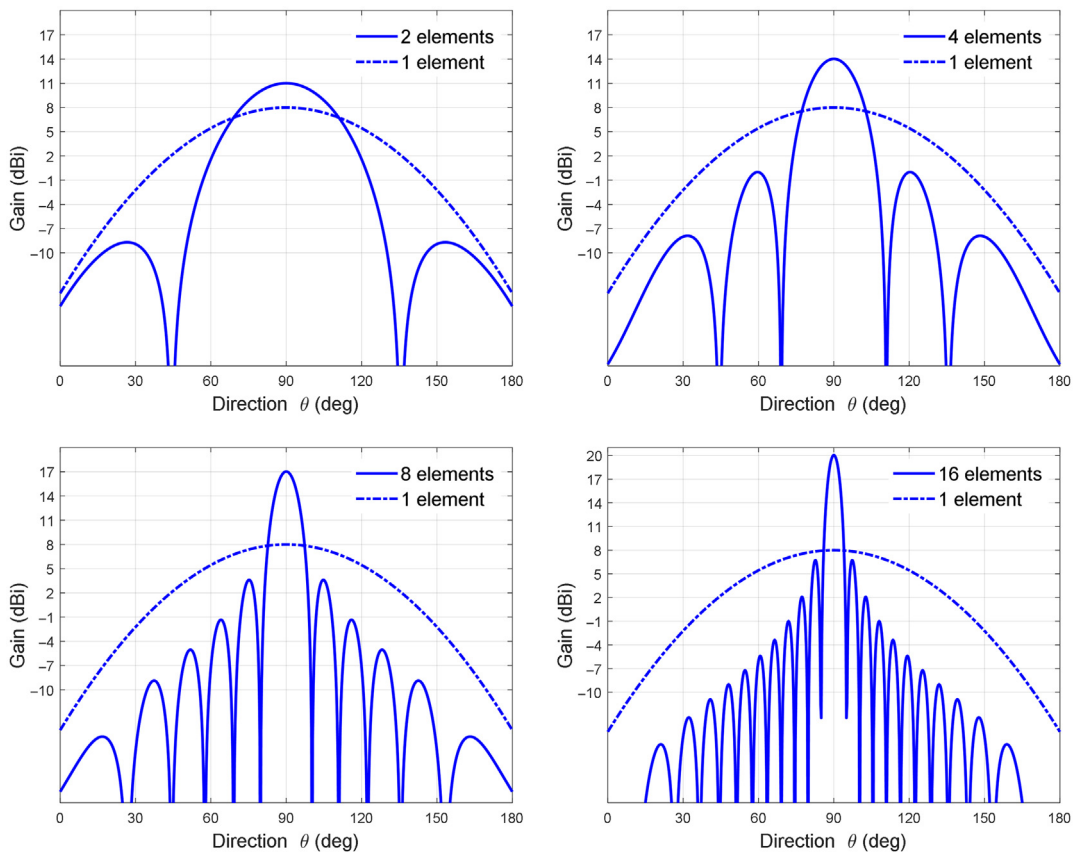
Illustration of gain pattern for horizontal arrays with two, four, and eight elements.

lobe in the corresponding dimension. Additionally, the gain patterns for the horizontal arrays are rotated versions of the corresponding vertical arrays and for this reason, only the case with vertical arrays is examined more closely in the following discussion.

To complement the three-dimensional illustrations of the gain patterns, Fig. 4.14 shows the gain pattern as a function of the zenith angle θ in the vertical plane $\varphi = 0^\circ$ for different vertical arrays.

As can be seen from Fig. 4.14, there is a peak as well as several nulls in the gain pattern. The width of the main lobe decreases and the number of nulls increases as the number of elements increases. To analyze this in somewhat more detail, the array factor is determined. Substitution of (4.47) and (4.46) into (4.44) results in

$$|\text{AF}(\theta, \varphi)|^2 = \left| \sum_{n=0}^{N-1} \frac{1}{\sqrt{N}} e^{jkd\cos\theta} \right|^2 = \frac{1}{N} \left| \frac{\sin(N \frac{kd\cos\theta}{2})}{\sin(\frac{kd\cos\theta}{2})} \right|^2 \quad (4.48)$$

**FIGURE 4.14**

Gain pattern as a function of θ for $\varphi = 0^\circ$ for vertical arrays with different number of elements.

where $k = 2\pi/\lambda$. The last equality follows from the fact that the sum is a geometric series (see also [1] for a detailed derivation). The observations done for the case with two elements in Section 4.2.4 are now generalized to the case with more elements:

- The maximum gain for an array with N elements is N times higher compared to a single element. Maximum gain occurs where all the elements' contributions are in phase, and this together with the element orientation explains the peak at broadside, $\theta = 90^\circ$. At broadside, coherent addition of N terms, each with an amplitude $1/\sqrt{N}$, results in a power gain of N in addition to the element gain. As can be seen in Fig. 4.14, for two elements, the gain as compared to a single element is 3 dB, for four elements it is 6 dB and in the general case, it is $10\log_{10} N$ dB.

- There are nulls in the gain pattern. A null occurs when all the contributions sum destructively so that the array factor becomes zero. From the expression for the array factor in (4.48), the first nulls occur when

$$N \frac{kd\cos\theta}{2} = \pm \pi \rightarrow d\cos\theta = \pm \frac{\lambda}{N}. \quad (4.49)$$

Here, $d\cos\theta$ can be recognized as the path length difference between two adjacent elements (see also Section 4.2.3), and it can be shown that there are nulls whenever this path length difference is a multiple of λ/N different from a multiple of the wavelength (see also [1]). This explains why the number of nulls increases with increasing number of elements and furthermore shows that it depends on the element separation d .

- The width of the main lobe decreases with increasing number of elements. More specifically, the width scales approximately with $\lambda/(dN)$ since the angular separation between the first nulls scales in this way for small $\lambda/(dN)$. This can be seen by first solving (4.49) to establish that the first nulls appear at angles $\pm \cos^{-1}(\lambda/(dN))$ and then use a Taylor expansion, $\cos^{-1}(\lambda/(dN)) \approx \pi/2 - \lambda/(dN)$. The reader is referred to [1] for more details as well as more exact expressions. It should though be remembered that the exact half-power main lobe width depends not only on the array factor but also on the element pattern, whereas the locations of the nulls do not. Although the nulls do not coincide with the directions corresponding to the half-power main lobe width, the scaling for the latter is nevertheless similar to the scaling of the width as measured between nulls.
- Thus, for fixed element separation, d , and wavelength, λ , the main lobe width scales with $1/N$. With reference to Figs. 4.12 and 4.13, it can be seen that vertical stacking of elements into a vertical array reduces the main lobe width in the vertical plane, whereas horizontal stacking of elements into a horizontal array reduces the main lobe width in the horizontal plane.

In summary, an array with N elements can increase the gain relative to a single element with N , or $10\log_{10}N$ dB on logarithmic scale. At the same time, the half-power beamwidth of the main lobe at broadside, which represents the range of angles where the gain is high, becomes narrower for a fixed element separation and scales approximately as $\lambda/(dN)$. Finally, it was also observed that there are nulls in the radiation pattern, which indicates that it is possible to not only improve the received signal power in a direction, it is also possible to reduce the signal power in other directions.

4.4 BEAMFORMING

So far, the same signal has been transmitted from all the elements and it has been demonstrated that by increasing the number of elements in the array the gain increases at broadside, at zenith angle $\theta = 90^\circ$ and azimuth angle $\varphi = 0^\circ$. At the same time, it was also seen that the width of the main lobe decreases when increasing the number of antennas in the array. In a cellular deployment, it is of interest to increase the signal strength not only at broadside but to terminals that may be at an arbitrary angle within a certain range. Beamforming allows adjusting the direction with

maximum gain, that is, the direction of the main lobe, and this adjustment can be done dynamically without changing the mechanical orientation of the array.

More specifically the direction is adjusted by changing the transmission delay of the signal copies transmitted from different elements so the contributions from the different elements arrive at the same time at the receiver and therefore combine constructively. Equivalently, for a narrowband signal this can be accomplished by applying a corresponding element-specific phase shift, and this is what the beamforming weight vector represents. Thus, the beamformer adjusts the phase of the transmitted signals so that they add in phase at a receiver in a certain direction. This means that the gain as compared to a single element, the free-space array gain, will be equal to N , the number of elements, not only at broadside but in any desired direction. Some illustrations of this will be given for a ULA, followed by a short discussion on element separation and so-called grating lobes.

The technique, to steer a beam in a certain direction by adjusting the phase of the transmitted signals to maximize the gain to a receiver in a certain direction, leads to what in the present book is referred to as classical beamforming. In Chapter 6, multiple antenna techniques including more advanced beamforming techniques are considered in the context of 5G radio network deployments. However, already here, the opportunities beyond classical beamforming are illustrated. By choosing the beamforming weights more flexibly, including also adjusting the amplitude, it is possible to suppress sidelobes, place nulls in certain directions and increase the width of the main lobe.

4.4.1 CLASSICAL BEAMFORMING

So far in the present chapter, the focus has been on the case that the same signal is transmitted from all the elements of the array. This is now revisited so that copies of the same signal but with different time delays are transmitted from the elements. For this purpose, the transmission time delay of the signal from antenna n is denoted $\tau_{t,n}$ where the subscript t refers to transmission. The intention is to choose the delays so that the signals add constructively at a receiver in direction θ_0 and φ_0 .

Furthermore, in the definition of the array response vector $\mathbf{a}(\theta, \varphi)$, which includes the impact of the propagation delay differences as function of direction, it was found (see (4.40)), that the relative propagation delay $\Delta\tau_n(\theta_0, \varphi_0)$ for element n satisfies

$$2\pi f_c \Delta\tau_n(\theta_0, \varphi_0) = -\mathbf{d}_n^T \mathbf{k}(\theta_0, \varphi_0). \quad (4.50)$$

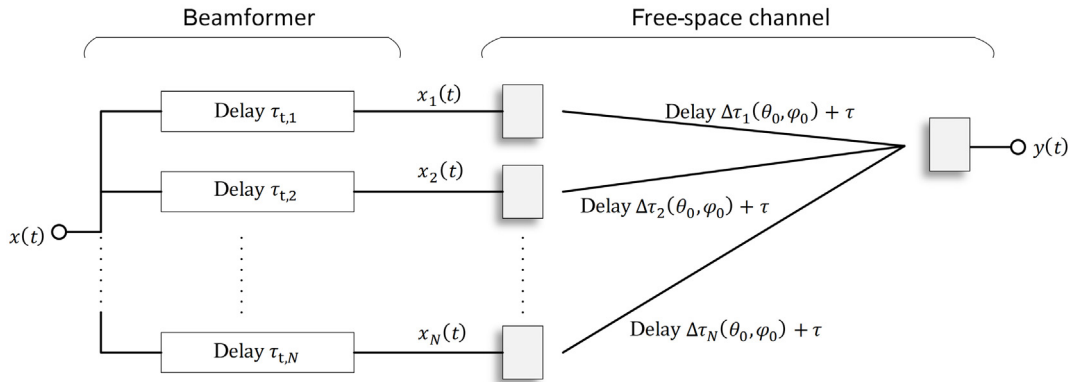
Thus, the propagation delay difference is related to path length difference which in turn is related to the position \mathbf{d}_n [see (4.27)], relative to a reference point as well as the direction of the receiver in terms of the wave vector $\mathbf{k}(\theta_0, \varphi_0)$ defined in (4.39).

In Fig. 4.15, the signal paths are illustrated. In the figure, also the delay between the array's reference point used to define the element positions, and the receiving antenna, τ , is included. The total delay for the contribution from element n is

$$\tau_{\text{tot},n} = \tau_{t,n} + \Delta\tau_n(\theta_0, \varphi_0) + \tau. \quad (4.51)$$

To make the contributions from the individual elements add constructively, the delays are chosen so that all the contributions have the same total delay. For this reason, they are chosen as

$$\tau_{t,n} = -\Delta\tau_n(\theta_0, \varphi_0) \rightarrow \tau_{\text{tot},n} = \tau \text{ for all } n = 1, \dots, N. \quad (4.52)$$

**FIGURE 4.15**

Copies of the same signal with different total delays reach the receiving antenna in the direction θ_0 and φ_0 .

In the example of Fig. 4.15, where an element further down the array with increasing index n has a longer propagation delay, the transmission delays should be chosen as $\tau_{t,1} > \tau_{t,2} > \dots > \tau_{t,N}$. Since the signal, $x(t)$ according to (4.8), is a complex baseband equivalent to a narrowband radio frequency signal $x_{RF}(t)$, a delay of the radio frequency signal corresponds to a phase shift of the baseband signal (see also Section 4.2.5),

$$x_{RF}(t - \tau_{t,n}) \leftrightarrow e^{-j2\pi f_c \tau_{t,n}} x(t). \quad (4.53)$$

This means that the baseband signal transmitted from element n is to be taken as

$$x_n(t) = w_n x(t), \quad n = 1, \dots, N, \quad (4.54)$$

where w_n is the complex weight associated with element n . To implement the time delay, the weight w_n is chosen as

$$w_n = \frac{1}{\sqrt{N}} e^{-j2\pi f_c \tau_{t,n}} = \frac{1}{\sqrt{N}} e^{j2\pi f_c \Delta\tau_n(\theta_0, \varphi_0)} = \frac{1}{\sqrt{N}} e^{-jd_n^T k(\theta_0, \varphi_0)}, \quad (4.55)$$

where (4.52) and (4.50) have been used and the factor $1/\sqrt{N}$ represents the fact that the total power is the same independent on how many elements are used. The weights of all the N elements are then collected into a beamforming weight vector, denoted $\mathbf{w}(\theta_0, \varphi_0)$ to stress its dependency on the steered direction (θ_0, φ_0) ,

$$\mathbf{w}(\theta_0, \varphi_0) = \frac{1}{\sqrt{N}} \begin{bmatrix} e^{-jd_1^T k(\theta_0, \varphi_0)} & e^{-jd_2^T k(\theta_0, \varphi_0)} & \dots & e^{-jd_N^T k(\theta_0, \varphi_0)} \end{bmatrix}^T. \quad (4.56)$$

The derivations of the gain done in Section 4.3.2 did not make any specific assumptions on the beamforming weight vector and therefore (4.43) still applies with the array response vector as

defined in (4.38). Using the expressions for the array response vector and the beamforming weights, the gain in the steered direction (θ_0, φ_0) becomes

$$G_{AA}(\theta_0, \varphi_0) = |\mathbf{a}^T(\theta_0, \varphi_0)\mathbf{w}(\theta_0, \varphi_0)|^2 = \left| \sum_{n=1}^N \frac{1}{\sqrt{N}} \right|^2 G(\theta_0, \varphi_0) = NG(\theta_0, \varphi_0), \quad (4.57)$$

where $G(\theta, \varphi) = |g(\theta, \varphi)|^2$ is the elements' gain pattern. Thus, the delays, or equivalently the phase shifts, make all the contributions sum up constructively. Considering (4.45), it furthermore follows that the (free-space) array gain, as given by the array factor indeed is as expected,

$$|\text{AF}(\theta_0, \varphi_0)|^2 = N. \quad (4.58)$$

The Cauchy–Schwartz inequality can be used to establish an upper bound on the gain for any choice of weights \mathbf{w} subject to the total power constraint $\|\mathbf{w}\|^2 = 1$

$$\begin{aligned} \|\mathbf{w}\|^2 &= 1, \|\mathbf{a}(\theta_0, \varphi_0)\|^2 = NG(\theta_0, \varphi_0) \\ \rightarrow G_{AA}(\theta_0, \varphi_0) &= |\mathbf{a}^T(\theta_0, \varphi_0)\mathbf{w}|^2 \leq NG(\theta_0, \varphi_0) \end{aligned}$$

Since the upper bound is achieved, it can be concluded that the choice of beamforming weights (4.56) does indeed maximize the gain in the direction θ_0 and φ_0 . This comes from the fact that the conjugates of the beamforming weights, $\mathbf{w}^c(\theta_0, \varphi_0)$, is a scaled version of the array response vector $\mathbf{a}(\theta_0, \varphi_0)$.

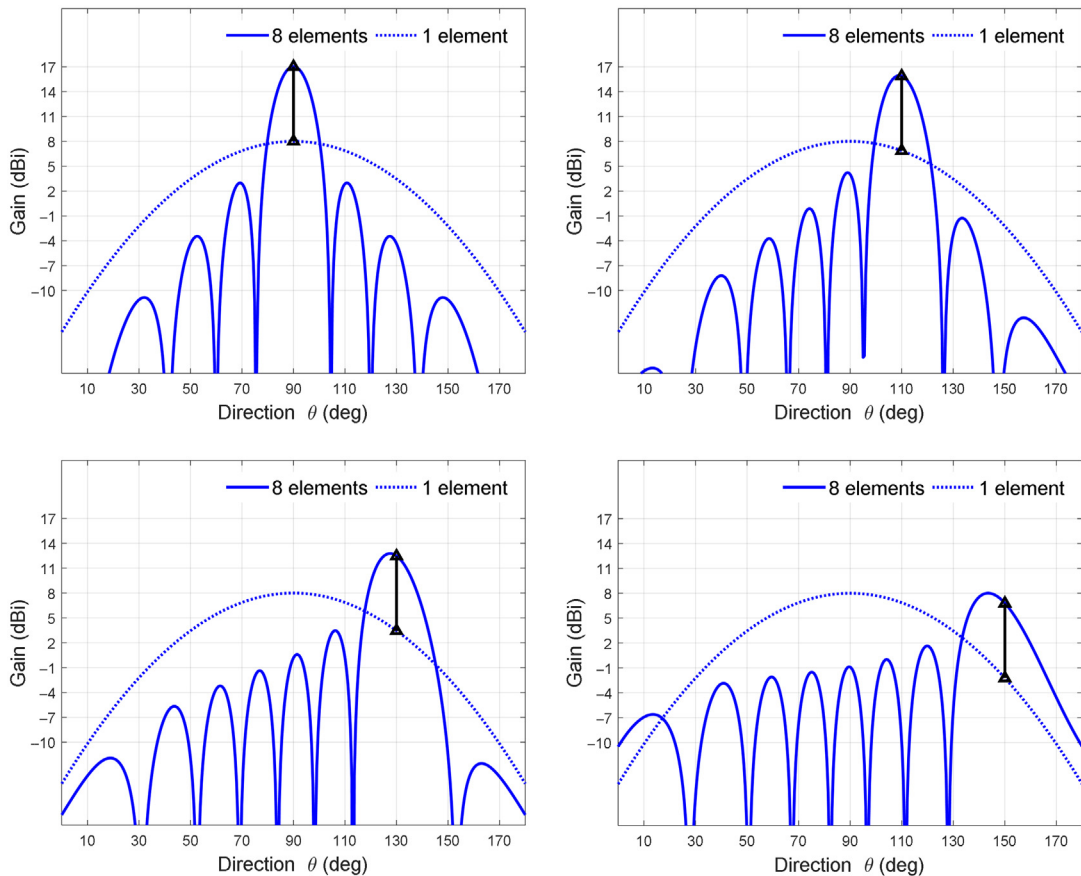
To sum up, the direction where the array gain pattern is maximized can be changed by adjusting the delays, or equivalently the phase shifts represented by the elements in the beamforming weight vector.

4.4.2 UNIFORM LINEAR ARRAYS

For the case with a ULA and the classical beamforming weights given by (4.56), it is possible to formulate an expression for the absolute value squared of the array factor similar to (4.48). For the case with a vertical array, the difference is that $\cos\theta$ is to be replaced by $\cos\theta - \cos\theta_0$, and the properties of the gain patterns discussed in Section 4.2.4 do therefore essentially carry over (see further [1–3]). One difference is though that the main lobe width also increases as the steering direction changes from broadside, $\theta_0 = 90^\circ$ and this will be seen in the examples below. Another difference is that the maximum gain, which includes both the array gain part and the element gain part, will not necessarily occur at the steered direction θ_0 . The reason for this is that the gain in a certain direction depends not only on the array factor but also on the element gain in that direction.

A specific example, with a vertical ULA as defined in Section 4.3.3, is considered. The array consists of $N = 8$ elements separated $d = 0.5\lambda$ with the element pattern defined in [6]. Four different steering angles θ_0 are considered and the gain pattern as a function of zenith angle θ for $\varphi = 0^\circ$ is shown in Fig. 4.16.

As can be seen, it is indeed possible to change the direction of the main lobe by adjusting the transmission timing of signal copies transmitted from different elements. It may also be observed that due to the element gain pattern, the direction in which the antenna gain of the array has its maximum does not fully coincide with the direction for which the array gain is maximized. Another impact of the element gain is that the maximum gain decreases with increasing steering

**FIGURE 4.16**

Gain pattern as a function of θ for $\varphi_0 = 0^\circ$ and four different steering directions $\theta_0 = 90^\circ$ (top left), $\theta_0 = 110^\circ$ (top right), $\theta_0 = 130^\circ$ (bottom left) and $\theta_0 = 150^\circ$ (bottom right) using an vertical array of eight elements with gain model according to [6] separated by $d = 0.5\lambda$. The black arrows represent the $10\log_{10}8 \approx 9$ dB where the array gain is maximized.

direction. However, the array gain is $10\log_{10}8 \approx 9$ dB for all the steered directions. Finally, the width of the main lobe increases as the angle between broadside and the steering direction increases.

In fact, since the gain in a given direction is the product of the corresponding element gain and the array gain, the envelope over all steered beams will have the same shape as the element pattern, and in the general case with N elements be $10\log_{10}N$ dB higher. This is illustrated in Fig. 4.17 where gain patterns for 20 different steering directions are shown.

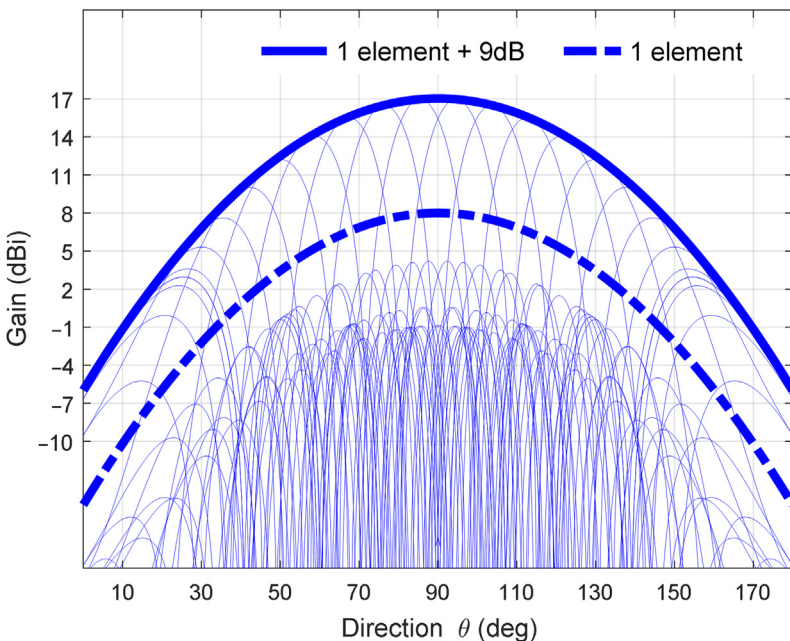


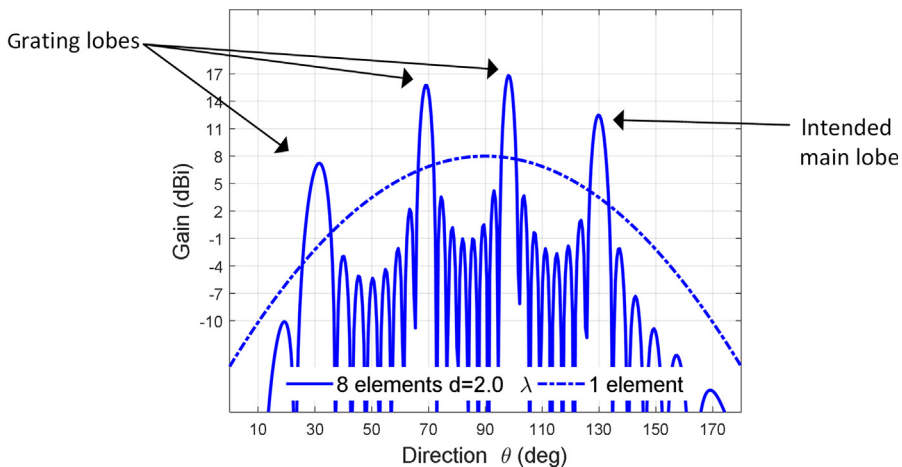
FIGURE 4.17

Gain pattern as a function of θ for $\varphi = 0^\circ$ and different steering directions θ_0 between 0° and 180° (thin lines) with a vertical array of $N = 8$ elements with gain model according to [6] and element separation $d = 0.5\lambda$. For comparison, the gain for a single element and the single element plus $10\log_{10}8 \approx 9$ dB are also shown.

4.4.2.1 On element separation

In the examples so far in the chapter, rather small element spacing has been considered, in the order of $0.5\lambda - 1.0\lambda$, since such are commonly used in practice. A detailed treatment of the impact of antenna separation would include accounting for the mutual coupling between the elements in the array and is beyond the scope of this book, even though some aspects are discussed in Section 12.3.7. However, common to many practical designs is that the maximum gain of the embedded pattern, which is different compared to the pattern of the element in isolation, can be increased when the spacing is increased. This appeals to intuition since a larger spacing would lead to a larger area per elements, which in turn allows collecting more incident power. Given a certain physical area, there is thus a choice between different partitioning in terms of number of elements and the area per element which corresponds to different array gains and element gains.

When designing an array, there are not only requirements on gain for signals transmitted to a single-intended user within a cell (for which it will become clear in Section 6.1.1.2 that the gain patterns may look substantially different as compared to the ones presented so far). There are also requirements to transmit signals with wider main lobes, for example intended to multiple users in a cell. Requirements here are not only related to gain and width of the main lobe but also related to

**FIGURE 4.18**

Gain pattern as a function of θ for vertical ULA with $N = 8$ elements separated by $d = 2\lambda$. The direction of the main lobe is steered to $\theta_0 = 130^\circ$.

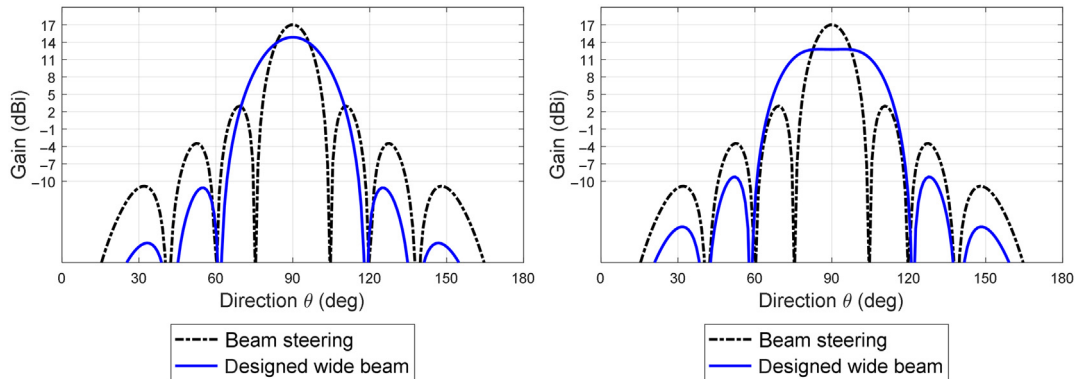
sidelobes. Balancing different requirements with cost, for example, in terms of antenna size and complexity, typically leads to antenna separations in the above-mentioned range with a bias toward $0.5\lambda - 0.7\lambda$.

As a side note, it is well known that increasing the element separation above 0.5λ leads to aliasing in the sense that so-called grating lobes as defined in [8] can occur (see also [3]). A rather extreme example of this is given in Fig. 4.18 for an element separation $d = 2\lambda$ and the main lobe steered to $\theta_0 = 130^\circ$. The corresponding case for 0.5λ is given in Fig. 4.16, where only the intended main lobe is present.

A grating lobe occurs in a direction other than intended direction in which the signals transmitted from all the elements combine constructively. This means that there is an ambiguity in the sense that the maximum array gain can be obtained in more than one direction. Whether ambiguity is a problem or not depends on the application, and if the application is to position a terminal by receiving signals in the uplink, it is indeed a problem since the direction cannot be uniquely determined. However, it is still possible to demodulate transmitted data.

4.4.3 BEAMFORMING BEYOND BASIC BEAM STEERING

In Section 4.4.1, basic beam steering was introduced, and it is illustrated in Section 4.4.2 that the direction of the main lobe could be steered to maximize the (free-space) array gain in a particular direction. More specifically, the beamforming weights are a function of the intended pointing direction which can be specified in terms of zenith and azimuth angles θ_0 and φ_0 . In the general case, the beamforming weights may be chosen more freely to generate quite arbitrary gain patterns. This is the topic of Chapter 6, in which multiple antenna techniques including beamforming techniques suitable for the multipath radio channels (cf. Section 6.1.1.2) are outlined. As will be seen there,

**FIGURE 4.19**

Examples gain patterns for two designed wide beams compared to the gain pattern with beam steering to $\theta_0 = 90^\circ$ for the case with vertical ULA with $N = 8$ elements.

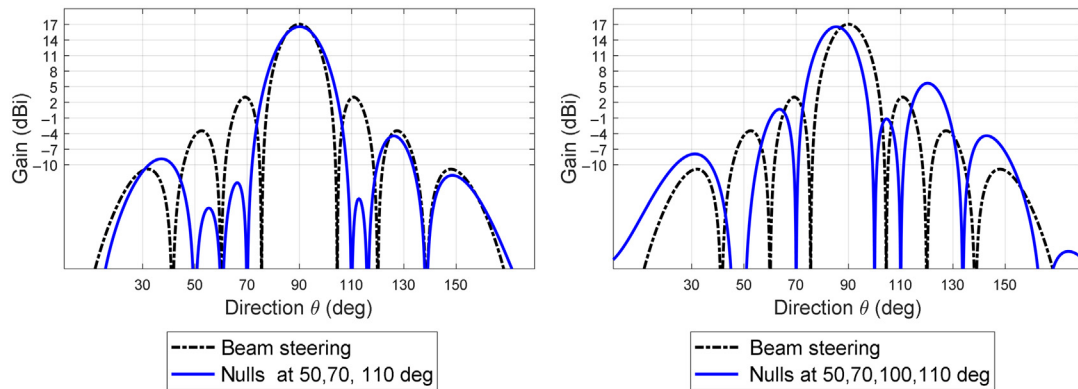
the gain patterns can have quite arbitrary shapes and different from the ones illustrated so far. Thus, in general, it is possible to select beamforming weights to obtain gain patterns with certain desired properties, for example, to suppress sidelobe levels, widening the main lobe or have nulls in specific directions. There is a vast literature available on the topic, and [1,3,9,10] can serve as starting points for further exploration. Here, the ambition is not to go through in detail how to generate beamforming weights to meet arbitrary gain patterns, but merely to make the reader aware of the fact that the properties of the gain pattern for basic beam steering as illustrated in Sections 4.2.4, 4.3.3.1, and 4.4.2 depend on how the beamforming weights are determined.

In Section 4.3.3.1, it was seen that the main lobe width for basic beam steering with a ULA decreases with increasing length of the array. However, if the beamforming weights are chosen differently, this needs not to be the case. For example, by choosing weights such that only one of the elements is used for transmission, then the main lobe width will not change. At the same time, there will not be any gain from using the array. In Fig. 4.19, gain patterns for two different beams designed with the Fourier transform method in [3] are shown for the same case as considered in Fig. 4.16, which is a vertical ULA with $N = 8$ elements separated by $d = 0.5\lambda$. The width of the main lobe is wider, but at the same time, the maximum gain is lower as compared to the beam steered to broadside $\theta_0 = 90^\circ$. In practice, there is often a constraint on maximum power per element, and for this reason other methods are used.

Another example includes creating nulls in the gain pattern in specific directions. For the case that the main lobe is steered to $\theta_0 = 90^\circ$, two directions with nulls are given by (4.49). To create nulls in L specific directions $\{(\theta_l, \varphi_l), l = 1, \dots, L\}$, the beamforming weights need to satisfy

$$\mathbf{a}^T(\theta_l, \varphi_l)\mathbf{w} = 0, \quad l = 1, \dots, L. \quad (4.59)$$

One interpretation of this is that weight vector, \mathbf{w} , is constrained to lie in the subspace defined by the constraints above, and one solution is to project the beamforming weight vector $\mathbf{w}(\theta_0, \varphi_0)$ defined in (4.56) onto this subspace. In practice, more sophisticated approaches are used to strike a balance between high gain in a desired direction and low but not necessarily zero gain in directions

**FIGURE 4.20**

Example of gain patterns with null steering compared to the gain pattern with beam steering to $\theta_0 = 90^\circ$ for the case with a vertical ULA with $N = 8$ elements.

to be nulled. For this reason, the details on the solution to (4.59) are not further elaborated here. In Fig. 4.20 gain patterns illustrating nulls being positioned in different directions are shown for the same setup as in Fig. 4.19.

To sum up, it is possible to create rather arbitrary gain patterns, and properties such as gain, and main lobe widths depend on the chosen beam weights. Typically imposing additional constraints in terms of nulls and beamwidth will lead to lower gain in the steered direction as compared to classical beamforming.

4.5 DUAL-POLARIZED UNIFORM PLANAR ARRAYS

The dual-polarized UPA is probably the most common array configuration being considered for advanced 4G and 5G systems. A UPA, also referred to as uniform rectangular array, offers the beamforming capabilities of both a vertical and a horizontal ULA simultaneously.

The UPA is a special case of the general array introduced in Section 4.2.5 with element positions on a uniform grid. For the basic beam steering technique introduced in Section 4.4.1 which aims at maximizing the gain in a certain direction, the array factor can be written as a product of an array factor for a vertical array and array factor for a horizontal array. The gain as compared to using a single element is therefore given by the total number of elements and at broadside, the vertical and horizontal width of the main lobe scales with the inverse of the size of the antenna in the corresponding dimension.

A dual-polarized UPA is a UPA of dual-polarized element pairs, more specifically two elements with different, preferably orthogonal, polarizations. The difference as compared to the case with co-polarized elements is that the beamforming vector generates weighted version of the signal to be transmitted to elements with different polarization. This allows not only changing the gain pattern but also controlling the polarization of the transmitted signals, for example to mitigate polarization mismatch (see also Section 3.4.2).

4.5.1 UNIFORM PLANAR ARRAY

A UPA consists of a number of elements arranged on a uniform grid with N_v rows and N_h columns. Such an array will be referred to as an $N_v \times N_h$ UPA and it contains in total $N = N_v N_h$ elements. The spacing between adjacent elements is d_v in the vertical domain and d_h in the horizontal domain and the spacing in the two domains need not be the same for the array to be referred to as a UPA. In Fig. 4.21 an example with an 8×4 UPA is depicted.

It may be noted that a ULA, as defined in Section 4.3.3, is a special case of a UPA. More specifically, a $1 \times N$ UPA corresponds to a horizontal ULA and an $N \times 1$ UPA is a vertical ULA.

The following assumptions are done:

- The $N = N_v N_h$ elements are ordered (see also Fig. 4.21) such that their locations in Cartesian coordinates are given by the vectors

$$\begin{aligned} \mathbf{d}_{1+m+nN_v} &= [0 \quad nd_h \quad md_v], \\ m &= 0, \dots, N_v-1, \\ n &= 0, \dots, N_h-1. \end{aligned}$$

- All elements have the same complex amplitude pattern $g(\theta, \varphi)$ oriented so that the maximum (magnitude) occurs in the direction of the x -axis, $\theta = 90^\circ, \varphi = 0^\circ$.

The assumption on the element pattern is further discussed in Section 4.3.3 and with reference to Fig. 4.21, the ordering of elements is when looking toward the array from the intended coverage area.

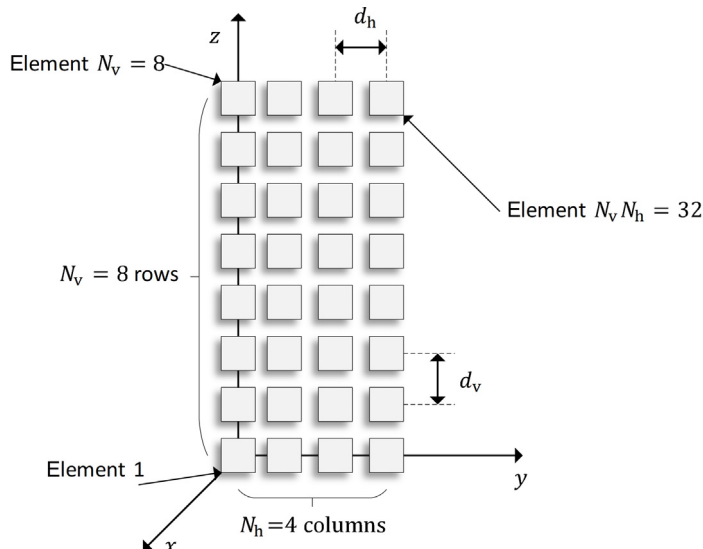


FIGURE 4.21

An 8×4 UPA with $N_v = 8$ rows and $N_h = 4$ columns.

4.5.1.1 Basic gain pattern

The UPA is a special case of an array with $N = N_v N_h$ elements, and under the assumptions listed in [Section 4.3.1](#), the array response vector can be determined from [\(4.38\)](#) based on the element positions in [\(4.60\)](#) as

$$[\mathbf{a}(\theta, \varphi)]_{1+m+nN_v} = g(\theta, \varphi) e^{j k m d_v \cos \theta} e^{j k n d_h \sin \theta \sin \varphi}, \quad (4.61)$$

for $m = 0, \dots, N_v - 1, n = 0, \dots, N_h - 1$. From [Section 4.4.1](#), it then follows that to maximize the gain in a direction θ_0 and φ_0 , the weights should according to [\(4.56\)](#) be selected as

$$[\mathbf{w}(\theta_0, \varphi_0)]_{1+m+nN_v} = \frac{1}{\sqrt{N_v}} e^{-j k m d_v \cos \theta_0} \frac{1}{\sqrt{N_h}} e^{-j k n d_h \sin \theta_0 \sin \varphi_0}, \quad (4.62)$$

for $m = 0, \dots, N_v - 1, n = 0, \dots, N_h - 1$. With the expression of the array response vector in [\(4.61\)](#) and the chosen beamforming weight vector [\(4.62\)](#), the gain pattern can be written as

$$G_{AA}(\theta, \varphi) = |\mathbf{a}^T(\theta, \varphi) \mathbf{w}(\theta_0, \varphi_0)|^2 = |\text{AF}_v(\theta, \varphi)|^2 |\text{AF}_h(\theta, \varphi)|^2 G(\theta, \varphi), \quad (4.63)$$

with

$$\text{AF}_v(\theta, \varphi) = \frac{1}{\sqrt{N_v}} \sum_{m=0}^{N_v-1} e^{j k d_v m (\cos \theta - \cos \theta_0)}, \quad (4.64)$$

$$\text{AF}_h(\theta, \varphi) = \frac{1}{\sqrt{N_h}} \sum_{n=0}^{N_h-1} e^{j k d_h n (\sin \theta \sin \varphi - \sin \theta_0 \sin \varphi_0)}. \quad (4.65)$$

Here, $\text{AF}_v(\theta, \varphi)$ is the array factor for a vertical ULA with N_v elements separated a distance d_v and $\text{AF}_h(\theta, \varphi)$ is the array factor for a horizontal ULA with N_h elements separated a distance d_h . The array factor can be factored into two array factors as in [\(4.63\)](#) as long as the beamforming weights are separable so that the weight for the element on row m of column n , $w_{m,n}$, can be written as $w_m w_n$. The beamforming weights in [\(4.62\)](#) are separable, and in that case, the UPA can be viewed in two ways:

- A vertical array where each element is a horizontal array so that $|\text{AF}_v(\theta, \varphi)|^2$ is the array gain pattern and $|\text{AF}_h(\theta, \varphi)|^2 G(\theta, \varphi)$ is the element gain pattern.
- A horizontal array where each element is a vertical array so that $|\text{AF}_h(\theta, \varphi)|^2$ is the array gain pattern and $|\text{AF}_v(\theta, \varphi)|^2 G(\theta, \varphi)$ is the element gain pattern.

For more details as well as further simplification of the array factors the reader is referred to for example [\[1\]](#).

From inspection of [\(4.63\)–\(4.65\)](#) it can be seen that the gain as compared to a single element obtained in the steered direction θ_0 and φ_0 is indeed equal to the total number of elements N . Furthermore, for ULAs it is seen in [Section 4.3.3](#) that for a main lobe at broadside, $\theta_0 = 90^\circ$ and $\varphi_0 = 0^\circ$, the width of the main lobe scales approximately as $\lambda/(Nd)$. As shown to the left in the example in [Fig. 4.22](#), the width of the main lobe is small in the vertical domain for an $N = 8$ vertical array whereas the width of the main lobe is small in the horizontal domain for a horizontal array. The right part of [Fig. 4.22](#) shows the gain pattern for an 8×8 UPA and the width of the main lobe in this case is reduced in both the horizontal and vertical domains.

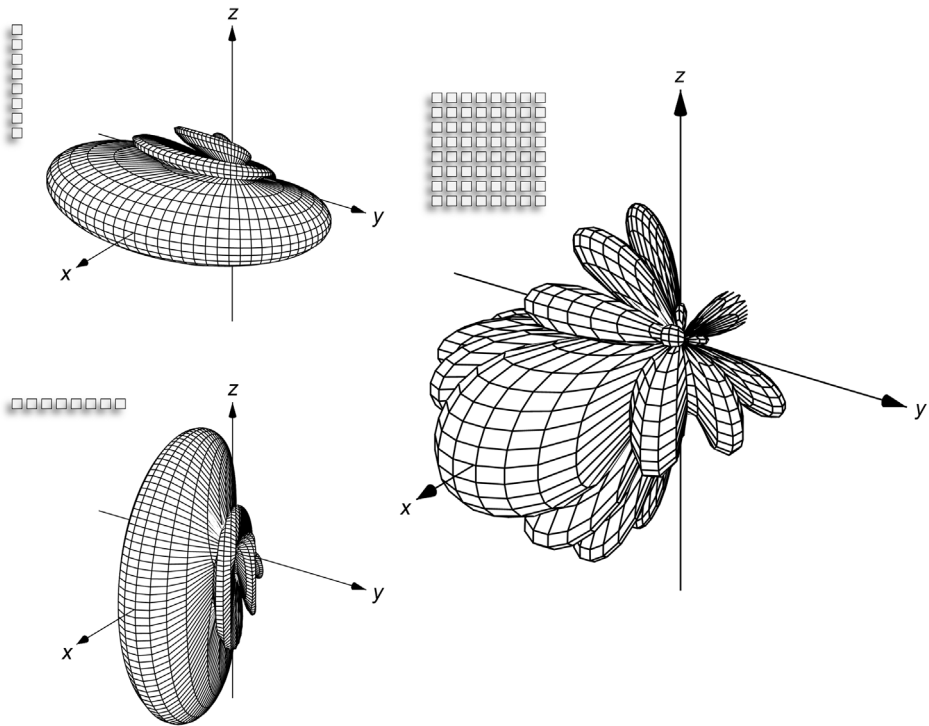
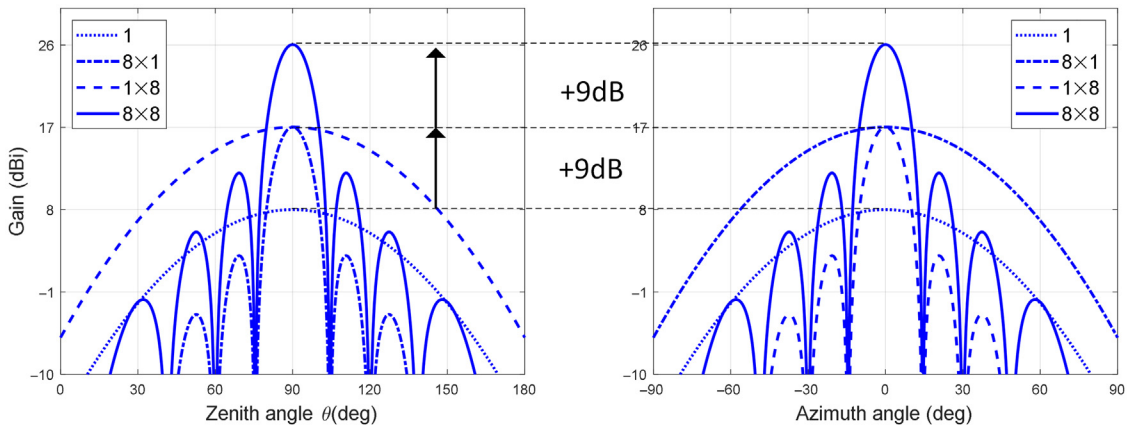
**FIGURE 4.22**

Illustration of gain pattern for an 8×8 UPA as well as vertical and horizontal ULAs with eight elements. The element is modeled according to [6], an element separation of $d = 0.5\lambda$ is assumed and the main lobe steered to toward broadside $\theta_0 = 90^\circ$ and $\varphi = 0^\circ$.

With a similar reasoning to that of [Section 4.3.3](#), it can be argued that the width of the main lobe decreases with the array size as $\lambda/(d_h N_h)$ in the horizontal domain and $\lambda/(d_v N_v)$ in the vertical domain for steering toward broadside. To illustrate this in more detail, the gain patterns, both as a function of the azimuth angle φ in the horizontal plane $\theta = 90^\circ$ and as a function of the zenith angle θ in the vertical plane $\varphi = 0^\circ$, are shown in [Fig. 4.23](#), for three different antennas arrays in addition to a single element. It may be noted that at broadside:

- Both a vertical array (8×1) and a horizontal array (1×8) offer $10\log_{10}8 \approx 9$ dB gain as compared to the single element.
- For the horizontal array (1×8) the main lobe is narrow in the horizontal plane, but as wide as the single element in the vertical plane.
- For the vertical array (8×1), the opposite is true in the sense that the main lobe is narrow in the vertical plane and wide in the horizontal plane.
- The 8×8 UPA offers another 9 dB over any of the two linear arrays, and the main lobe widths are narrow in both the vertical and horizontal planes.

**FIGURE 4.23**

Gain pattern as a function of zenith angle θ for $\varphi = 0^\circ$ (left) and as function of azimuth angle φ for $\theta = 90^\circ$ (right) for a single element (1), a vertical eight-element array (8×1), a horizontal eight-element array (1×8) and an 8×8 UPA (8×8). In all cases the element gain model in [6] is used, the element separation is $d = 0.5\lambda$ and the main lobe is steered to broadside.

To sum up, for basic beam steering with a UPA, the array factor can be factored into an array factor for a horizontal array and an array factor for a vertical array. The gain as compared to a single element is still given by the total number of elements. For a main lobe steered to broadside, the main lobe widths in the horizontal and vertical planes will however decrease inversely with increasing antenna size in the corresponding dimension.

4.5.2 DUAL-POLARIZED ARRAYS

Dual-polarized antennas have been used for a long time in radio access networks, both at the terminal side as well as on the base station side. On the base station side, multiple antennas were of interest initially to mitigate fading dips by diversity as well as losses due to polarization mismatch between transmitter and receiver antennas. More recently a key driver is to support spatial multiplexing as described in Section 6.3. The benefits of dual-polarized antennas can be leveraged also with antenna arrays, by using arrays of dual-polarized element pairs.

So far in the chapter, all the elements of the array have been assumed to have the same polarization, and to create a dual-polarized array, each element, such as a dipole, patch or Vivaldi element, is paired with an identical element with an as orthogonal polarization as possible (see also [3]). Often such dual-polarized element pairs are implemented in an area-efficient way. From the discussion in Section 4.4.2.1, with an assumed element spacing of around $0.5 - 1\lambda$, an element pair can conceptually be envisioned to be implemented within a square with such a side length. Most often an element pair with $\pm 45^\circ$ linear polarization is used, for example with a crossed dipole pair or a patch with two feed ports.

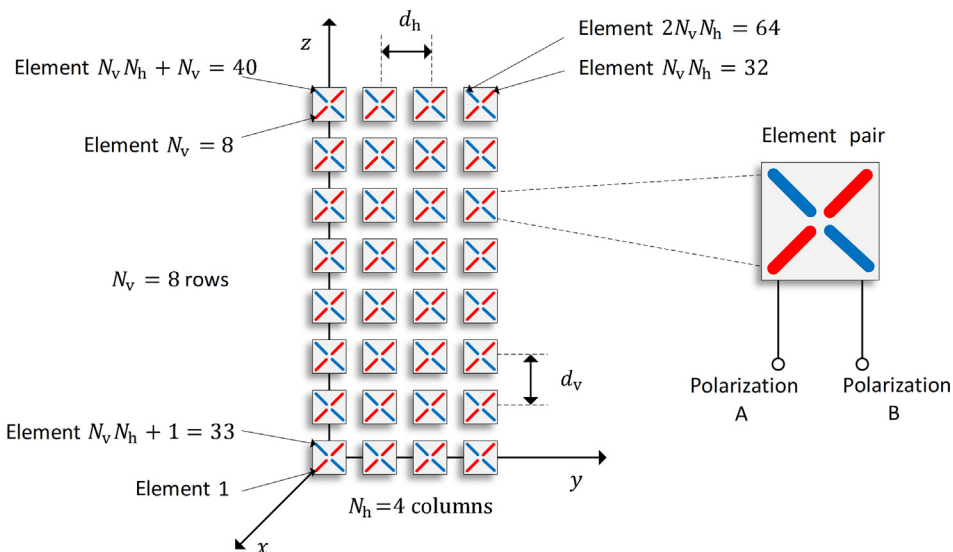


FIGURE 4.24

Example with uniform planar array of dual-polarized element pairs (left) and a single dual-polarized element pair (right).

In Fig. 4.24, a dual-polarized element pair is illustrated in addition to a UPA of dual-polarized element pairs. Each pair consists of two elements and has two ports, or feeds, one for polarization A and one for polarization B, that can be used for transmission and reception of signals implying that an $N_v \times N_h$ dual-polarized UPA has in total $N = 2N_v N_h$ elements.

Unless otherwise mentioned, the reader can assume that the N elements are ordered such that the first $N/2$ elements have a first polarization A and the last $N/2$ elements have a second polarization B. Moreover, the following can also be assumed:

- The $N = 2N_v N_h$ elements in the array are ordered (see Fig. 4.24) such that the locations of them in Cartesian coordinates are given by the vectors

$$\mathbf{d}_{1+m+nN_v+pN_v N_h} = [0 \quad nd_h \quad md_v], \quad m = 0, \dots, N_v - 1, n = 0, \dots, N_h - 1, p = 0, 1 \quad (4.66)$$

where p enumerates the two polarizations.

- All elements have the same complex amplitude pattern $g(\theta, \varphi)$ oriented so that the maximum (magnitude) occurs in the direction of the x -axis, $\theta = 90^\circ, \varphi = 0^\circ$.
- The elements' polarizations are defined as

$$\hat{\psi}_p(\theta, \varphi) = \begin{cases} \hat{\psi}_A(\theta, \varphi) & p = 1, \dots, N_v N_h \\ \hat{\psi}_B(\theta, \varphi) & p = N_v N_h + 1, \dots, 2N_v N_h \end{cases}, \quad (4.67)$$

where $\hat{\psi}_A(\theta, \varphi)$ and $\hat{\psi}_B(\theta, \varphi)$ represent the two polarizations (see also Section 3.3.3) which in the general case depend on direction, and not necessarily are orthogonal for all directions.

Assumptions on the element pattern are further discussed in [Section 4.3.3](#). Furthermore, recall from Sections 3.3.3 and 3.3.4 that the product $g(\theta, \varphi)\hat{\psi}_p(\varphi, \varphi)$ characterizes the transmitted wave in the far-field in terms of the two orthogonal $\hat{\theta}$ and $\hat{\varphi}$ components.

4.5.2.1 Beamforming including polarization

The use of an array with dual-polarized element pairs allows to control the polarization. This can be done with a beamformer that transmits the same signal with appropriate weights from two elements with orthogonal polarizations (see also [Section 3.2.3](#)). In the case with dual-polarized element pairs, such a beamformer could operate on element pairs effectively making each dual-polarized element pair appear as single element. This is illustrated in [Fig. 4.25](#).

In the example, the elements pairs are assumed to be $\pm 45^\circ$ linearly polarized. More specifically, it is assumed the polarizations in [\(4.67\)](#) in a particular direction, such as right in front of the element pairs, are given by

$$\hat{\varphi}_A = \frac{1}{\sqrt{2}}\hat{\theta} + \frac{1}{\sqrt{2}}\hat{\varphi}, \hat{\varphi}_B = \frac{1}{\sqrt{2}}\hat{\theta} - \frac{1}{\sqrt{2}}\hat{\varphi}. \quad (4.68)$$

Transmitting the same signal from both elements (left part of the figure) makes the element pair appear as to have vertical linear polarization whereas the other weighting (right part of the figure) makes the pair appear as an element with horizontal polarization. To be a bit more specific, consider a single dual-polarized element pair, that is, a UPA with $N_v = N_h = 1$, and assume similar to the case in [Section 4.2](#), that the same signal is transmitted from the two elements with weights w_1 and w_2 . Then the element pair will appear as an antenna with polarization $\hat{\psi}_t = w_1\hat{\psi}_A + w_2\hat{\psi}_B$ and this allows to minimize the loss due to polarization misalignment between transmitter and receiver antennas by appropriately adjusting w_1 and w_2 (see also [Section 3.4.2](#)). So far in the chapter, the polarizations have been assumed to be aligned (see [\(4.14\)](#)), and with dual-polarized element pairs, this can thus be achieved. Furthermore, it can also be combined with a UPA of arbitrary size, including a ULA, which is illustrated in [Fig. 4.26](#).

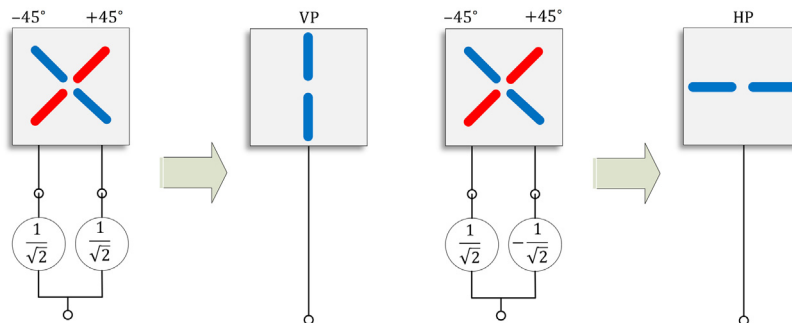
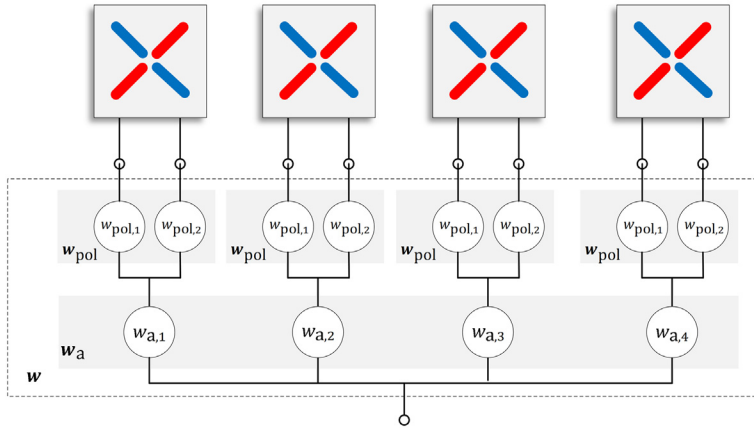


FIGURE 4.25

Beamforming with a $\pm 45^\circ$ linearly polarized element pair can appear as an element with for example vertical polarization (left) or horizontal polarization (right)

**FIGURE 4.26**

Example of beamforming with a dual polarized array where w_a is selected to steer a beam in a direction θ_0 and φ_0 , and w_{pol} is selected to control the polarization.

In Fig. 4.26, there are two beamformers. A first beamformer, w_a , is selected to steer a beam in a certain direction (θ_0, φ_0) for the UPA of element pairs. The second beamformer, w_{pol} , is then selected to control the polarization. It should be noted that in the general case, the N coefficients of a beamforming weight vector w can be freely chosen, and that the order of the beamformers can be exchanged. The purpose with the example is merely to demonstrate the possibilities offered by a dual-polarized array. Additional possibilities, more specifically, use of dual-polarized antennas for spatial multiplexing will be discussed in Section 6.3.

4.6 ARRAYS OF SUBARRAYS

To transmit a signal with beamforming, copies of the signal weighted according to the beamforming weight vector need to be generated for all the elements. For classical beamforming, this results in a narrower main lobe as compared to using a single element and allows the direction of the main lobe to be steered. If, however, the set of needed steering directions fall within a limited range of angles, it is not necessary to apply individual adjustments for all the elements. The array can be partitioned into *subarrays*, where a subarray is here defined for a dual-polarized antenna array as a subset of dual-polarized elements pairs connected to two ports, one for each polarization. To change the direction, a copy is then needed only for every subarray port. As will be seen, the range of angles, where the main lobe can be directed without significant gain drop, typically decreases by increasing the size of each subarray. For a given total array size, this corresponds to reducing the number of subarrays and thereby reducing the complexity in the sense that the number of signals that needs to be independently weighted is lower (see also Section 12.3.3).

In the present book, a subarray partitioning will refer to an implementation at radio frequency through appropriate design of the signal paths between a subarray's port and its elements. A radio chain is connected to each subarray port and since the number of radio chains needed can then be reduced, it enables a substantial complexity reduction. Therefore, the subarray size is an important design parameter for practical advanced antenna system (AAS) deployments and will be dealt with in Chapters 13 and 14 in general and in Section 13.2.2 in particular.

In what follows, partitioning of a UPA into subarrays is first defined, and after that gain as a function of angle will be illustrated for partitioning a vertical ULA into different subarray sizes.

4.6.1 PARTITIONING AN ANTENNA ARRAY INTO AN ARRAY OF SUBARRAYS

It is assumed that the array to be partitioned is a UPA with K_v rows and K_h columns of in total $K = K_v K_h$ dual-polarized element pairs as defined in [Section 4.5.2](#). The element pairs of such a UPA can be partitioned into non-overlapping rectangular subsets of element pairs, referred to as subarrays similar to [8]. All subarrays are, to ease the exposition, assumed to have the same size with M_v rows and M_h columns. Due to this the array can also be seen as an array of subarrays (AoSA), with N_v rows and N_h columns. Two examples of partitioning an 8×8 UPA of dual-polarized element pairs are shown in [Fig. 4.27](#).

Due to the assumption that subarrays have the same size, it follows that the dimensions of the subarray (M_v and M_h), the AoSA (N_v and N_h), and the underlying UPA (K_v and K_h) are related as follows

$$K_v = N_v M_v, K_h = N_h M_h.$$

In the following, the notation

$$(M_v \times M_h)_{\text{SA}}(N_v \times N_h)$$

will be used as shorthand for a UPA with N_v rows and N_h columns of subarrays with M_v rows and M_h columns.

Since the subarray is a UPA with dual-polarized element pairs, it is here defined to have a pair of ports, one for each polarization. This is different from [8] where a subarray has one port.

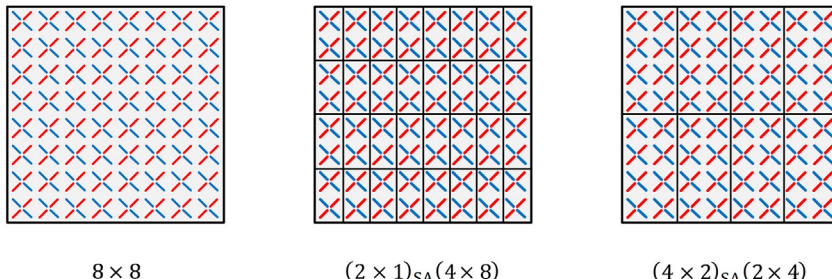


FIGURE 4.27

An 8×8 UPA with 64 dual-polarized element pairs (a) can, for example, be partitioned into a 4×8 array of subarrays with 2×1 subarrays (b) or into a 2×4 array of subarrays with 4×2 subarrays (c).

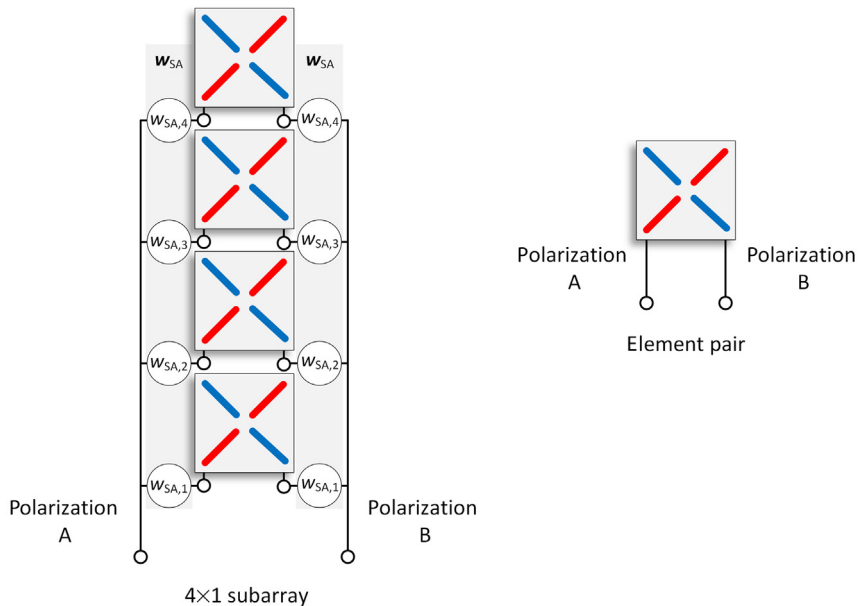


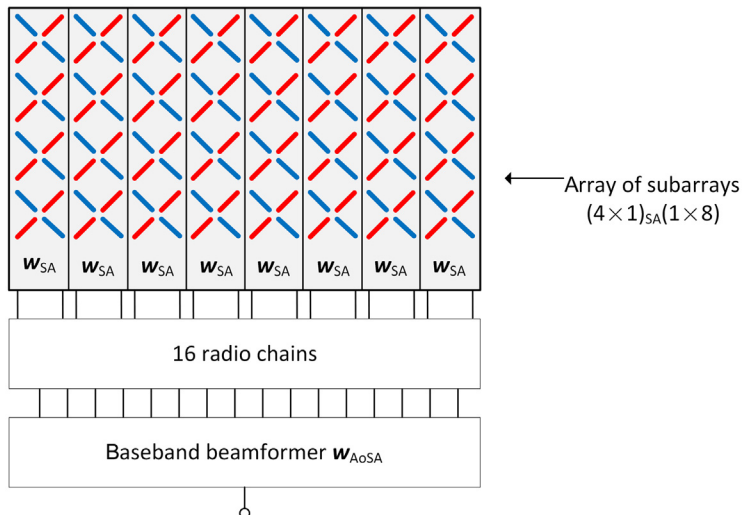
FIGURE 4.28

Example of a 4×1 subarray (left) consisting of four dual-polarized element pairs (right).

More specifically, an element pair has one element with polarization A and one element with polarization B. In line with this, the subarray has two ports, one for polarization A and another for polarization B. The elements with polarization A are connected to the subarray port with polarization A and the elements with polarization B are connected to the subarray port with polarization B.

Furthermore, a radio chain is connected to a subarray port and the signal transmitted from an element will depend also on the phase characteristics of the signal path between the subarray port and the element. If all signal paths are such that exactly the same signal is transmitted from the elements of the subarray, the gain will increase at broadside (see Sections 4.3.2 and 4.5.1.1). At the same time, it is also possible to design other characteristics for example by selection of signal paths' lengths', or equivalently phase shifts (see Section 4.4.1) to adjust the direction of the main lobe, similar to electrical tilt in conventional base station antennas. In any case, this means that the signal paths' characteristics of the subarray can be represented by a classical beamformer, w_{SA} , which in what follows, is assumed to be the same for both polarizations and also fixed in the sense that it is not dynamically changed to steer beams to different users in different time slots. The functionality of a subarray is illustrated with an example in Fig. 4.28.

From a radio perspective, the array of subarrays appears as a UPA of dual-polarized element pairs, where in this case each element pair is a subarray. This means that the radio needs to have in total $2N_v N_h$ radio chains, one per subarray port and weighted versions of the signal are generated based on the beamforming weight vector w_{AoSA} which can be dynamically changed. This is illustrated in Fig. 4.29.

**FIGURE 4.29**

Example with beamforming at baseband seeing a 1×8 UPA of dual-polarized subarrays, converted to radio frequency using 16 radio chains and connected to a 4×8 UPA partitioned into a 1×8 array of subarrays with 4×1 subarrays.

The total beamforming weight vector as seen from the array of dual-polarized element pairs is thus the result of both the subarray beamformer w_{SA} and the beamformer realized by the radio w_{AoSA} . Whereas the radio chains allow to dynamically adapt the beamformer w_{AoSA} , the subarray beamformer w_{SA} is implemented at radio frequency close to the antenna elements and regarded as either fixed or changed on a slow basis for electrical down-tilt functionality. Thus, effectively, the set of beamforming weights that can be used for the array of element pairs is constrained.

In previous sections, it has been established that the total gain is a function of the elements' gain and the array gain and that the array gain for classical beamforming is given by the number of elements. In the present case, the subarray can be seen as an element, and when an AoSA is used with classical beamforming, the achievable gain pattern will have the same shape as the subarray pattern, similar to Fig. 4.17. Since the subarray beamformer is taken as a classical beamformer, with main lobe width decreasing with increasing subarray size, it follows for a fixed array size that the range of angles with high total gain decreases as the subarray size increases, or equivalently, as the number of radio chains is reduced.

Finally, it should also be noted that the concept of subarrays as described in here can be generalized, for example, to allow dynamic updating of the subarray beamformer weights but in a constrained manner such as constant over frequency in case of OFDM-based transmission introduced in Chapter 5. Such a generalization can be viewed as offering the possibility to dynamically change the intended coverage area within which the AoSA beamformer may operate completely flexible over also frequency. A detailed description of this is however beyond the scope of this book.

4.6.2 GAIN PATTERNS

To illustrate the impact of the subarray partitioning introduced in the previous Section 4.6.1, classic beamforming is considered. Only one of the polarizations is examined, and the receiver antenna is assumed to be aligned with respect to the chosen polarization. From the radio's perspective the AoSA then appears as an $N_v \times N_h$ UPA where each element is a subarray which in turn appears as an $M_v \times M_h$ UPA. The gain as a function of direction can therefore be expressed using (4.63) as

$$G_{\text{AoSA}}(\theta, \varphi) = |\text{AF}_v(\theta, \varphi)|^2 |\text{AF}_h(\theta, \varphi)|^2 G_{\text{SA}}(\theta, \varphi), \quad (4.69)$$

$$G_{\text{SA}}(\theta, \varphi) = |\text{AF}_{v,\text{SA}}(\theta, \varphi)|^2 |\text{AF}_{h,\text{SA}}(\theta, \varphi)|^2 G(\theta, \varphi). \quad (4.70)$$

The array factors for the AoSA, $\text{AF}_v(\theta, \varphi)$, and $\text{AF}_h(\theta, \varphi)$ are given by (4.64) and (4.65) with element spacing $M_v d_v$ and $M_h d_h$, respectively, and they depend on the dynamically controlled steering direction θ_0 and φ_0 . The same expressions also apply for the subarray's array factors $\text{AF}_{v,\text{SA}}(\theta, \varphi)$ and $\text{AF}_{h,\text{SA}}(\theta, \varphi)$, but with element spacing d_v and d_h , respectively, and corresponding fixed or slowly varying steering directions θ_{SA} and φ_{SA} for the subarray.

In any steered direction θ_0 and φ_0 , the array factors for the AoSA will achieve their maximum values, so that (4.69) becomes

$$G_{\text{AoSA}}(\theta_0, \varphi_0) = N_v N_h G_{\text{SA}}(\theta_0, \varphi_0), \quad (4.71)$$

and for the special case that the steered direction coincides with the fixed subarray steering direction, $\theta_0 = \theta_{\text{SA}}$ and $\varphi_0 = \varphi_{\text{SA}}$, the gain in (4.71) becomes using (4.70)

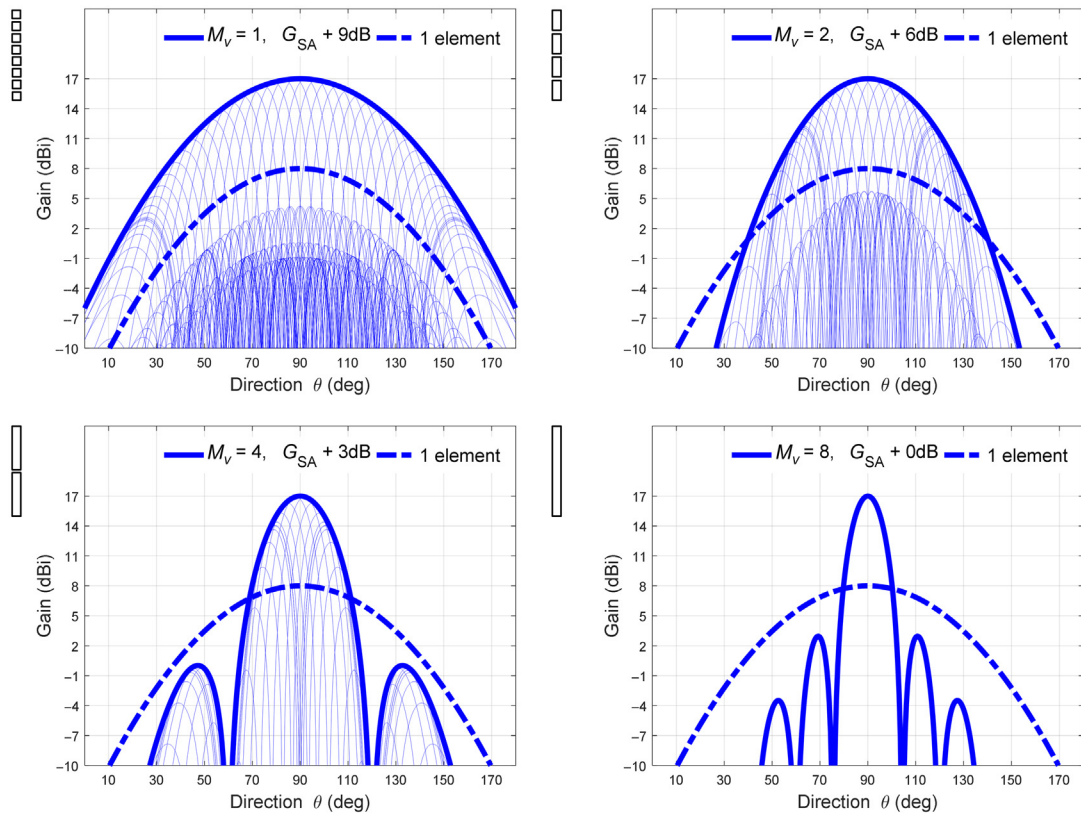
$$G_{\text{AoSA}}(\theta_{\text{SA}}, \varphi_{\text{SA}}) = N_v N_h M_v M_h G(\theta_{\text{SA}}, \varphi_{\text{SA}}). \quad (4.72)$$

Thus, in the direction of the subarrays' steered direction, the gain over using a single element is given by the total number of element pairs in the partitioned array $K = N_v N_h M_v M_h$. This is the same as the maximum gain obtained if the subarray constraint would be lifted so that there was one radio chain per element. Thus, the subarray partitioning does not reduce the maximum gain.

From (4.71) it further follows that the shape of the achievable gain pattern, which is the envelope of all steered beams, is given by the subarray gain pattern, which in turn depends on the size of the array in the corresponding dimension (see also Section 4.5.1.1). Taking the case when the subarray is a vertical ULA, the following is noted:

- The taller the subarray, the smaller is its vertical half-power beamwidth and the smaller is the range of elevation angles for which a gain within say 3 dB of the maximum gain can be achieved. At the same time, for a fixed total array size, the taller the subarray, the lower is the number of subarrays and the lower is the number of radio chains needed.
- The shorter the subarray, the larger is its vertical half-power beamwidth and the larger is the range of elevation angles for which a gain within say 3 dB of the maximum gain can be achieved. At the same time, for a fixed total array size, the shorter the subarray, the higher is the number of subarrays and the higher is the number of radio chains needed.

This is next further explored for an 8×1 vertical UPA. Such a UPA can be partitioned in four different ways with subarray sizes 1×1 , 2×1 , 4×1 , and 8×1 with corresponding AoSA sizes 8×1 , 4×1 , 2×1 , and 1×1 where the case $(8 \times 1)_{\text{SA}}(1 \times 1)$ corresponds to the case with no

**FIGURE 4.30**

Gain pattern as a function of θ for different steering angles θ_0 between 0° and 180° (thin lines) by using a vertical array of $K_v = 8$ elements with gain model according to [6], element separation $d = 0.5\lambda$, and different subarray sizes M_v with $\theta_{SA} = 90^\circ$. For comparison, the gain for a single element and the gain for a single subarray plus $10\log_{10}N_v/M_v$ are also shown.

dynamic beamforming. Gain pattern as a function of the angle θ for $\varphi = 0^\circ$ is plotted for different steering angles θ_0 and for comparison the envelope of the steered main lobes, as given by (4.71), is plotted as well in Fig. 4.30.

Another perspective is given in Fig. 4.31, showing the gain pattern for the individual subarrays to the left, and further the envelopes for the different subarray sizes when used with beamforming to the right. Such an envelope, or achievable gain thus includes both gain of the subarrays' fixed beamformer as well as the gain of dynamic beam steering.

To sum up, the gain for beamforming using a UPA partitioned into AoSA has been considered, and it was illustrated that the range of angles for which high gain can be offered, for example to match an intended coverage area, depends on the size of the subarrays. If the range of angles is small, it is possible to use large subarrays, which, as further discussed in Section 12.3.3, offer cost-efficiency benefits.

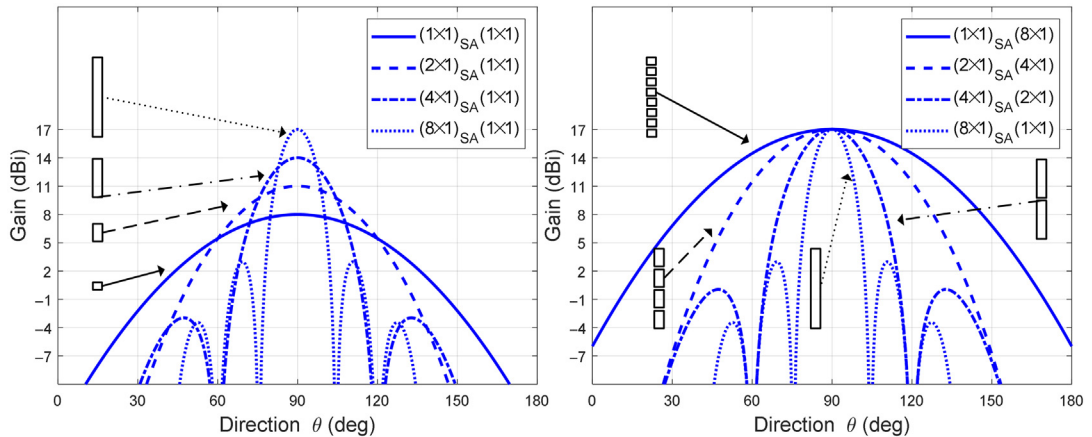
**FIGURE 4.31**

Illustration of gain pattern for a single subarray (left) and the envelope of all beams when beam steering is done using the array of subarrays (right).

Finally, the selection of a suitable antenna configuration needs to consider both the signal gain and interference, and this topic is addressed in Sections 13.4 and 14.3, where it is demonstrated that a suitable array partitioning depends on the deployment. Typically, such partitioning is done in the vertical domain since the range of vertical angles as seen from the base station is rather small. In this case, the partitioning allows benefiting from the antenna area without requiring an excessive number of radio chains.

4.7 SUMMARY

As stated in the introduction, the intention with this chapter is to explain the basic concept of classical beamforming. Similar to a flashlight beam, signal power can be directed in a desired direction and this has been illustrated in the form gain patterns for uniform linear and planar arrays.

A summary of the chapter is as follows.

- Classic beamforming is described in [Section 4.4.1](#).
 - It can maximize the gain pattern in a steerable direction under free-space propagation conditions.
 - With an array of N elements, the gain in terms of received power compared to using a single element is N in the steered direction for the case of free-space propagation.
 - The power gain as compared to a single isotropic antenna in any steered direction is a product of N and the elements' gain in the steered direction.
 - For a ULA, the width of the main lobe steered to broadside is approximately proportional to $\lambda/(dN)$ in the dimension of the array's orientation, where λ is the wavelength and d is the element separation.

- For a UPA, the width of the main lobe steered to broadside in the vertical and horizontal domain is proportional to main lobe widths of the corresponding vertical and horizontal linear arrays.
- Gain and width of the main lobe depend not only on the array but also on the beamformer as illustrated in [Section 4.4.3](#).
- Array configurations
 - A uniform linear array (ULA) is defined in [Section 4.3.3](#).
 - A uniform planar array (UPA) is defined in [Section 4.5.1](#).
 - A UPA of dual-polarized element pairs is defined in [Section 4.5.2](#). This array configuration allows the beamformer to control also the polarization as illustrated in [Section 4.5.2.1](#).
- The array response vector $\mathbf{a}(\theta, \varphi)$ is defined in [Section 4.3.2](#).
 - It includes the elements' amplitude pattern and the phase shift due to propagation delay differences as a function of direction for the elements of the array.
 - It can be seen as a free-space channel between the transmitting elements of the array and an isotropic receiving antenna as function of direction.
 - It will be used in [Section 5.3.2](#) to formulate a MIMO channel model.
 - The gain in a certain direction can be expressed as a product between the corresponding array response vector and the beamforming weight vector.
- Arrays of subarrays
 - An array can be partitioned into subarrays with fixed beamformers as described in [Section 4.6.1](#).
 - Such a partitioning allows a tradeoff between the number of radio chains and the range of angles for which high gain can be achieved. This concept is used when identifying suitable AAS configurations for different deployment scenarios in Chapters 13 and 14.

In Chapters 5 and 6, the discussion will be extended beyond classical beamforming, free-space propagation and multiple antennas only at the transmitter side. More advanced multiple antenna techniques will be considered for OFDM-based transmission in multipath propagation scenarios with multiple antennas also at the receiver side.

REFERENCES

- [1] C.A. Balanis, *Antenna Theory: Analysis and Design*, 3rd ed., John Wiley & Sons, 2005.
- [2] D.K. Cheng, *Field and Wave Electromagnetics*, 2nd ed., Pearson Higher Education, 1989.
- [3] R.J. Mailloux, *Phased Array Antenna Handbook*, 2nd ed., Artech House, 2005.
- [4] D. Tse, P. Viswanath, *Fundamentals of Wireless Communication*, Cambridge University Press, 2005.
- [5] J.G. Proakis, *Digital Communications*, 4th ed., McGraw-Hill, 2001.
- [6] 3GPP TR 38.901, V15.1.0. (2019-09) Study on channel model for frequencies from 0.5 to 100GHz.
- [7] H. Krim, M. Viberg, *Two decades of array signal processing: The parametric approach*, *IEEE Signal Processing Magazine* 13 (4) (April 1996).
- [8] IEEE standard for definitions of terms for antennas, IEEE Std 145-2013, 2013.
- [9] B.D. Van Veen, K.M. Buckley, *Beamforming: a versatile approach to spatial filtering*, *IEEE ASSP Mag*. 5 (2) (1988).
- [10] L.C. Godara, *Application of antenna arrays to mobile communications, Part II: Beam-forming and direction-of-arrival considerations*, *Proc. IEEE* 85 (8) (1997).